Article

Cell Reports

Neurons Differentiated from Transplanted Stem Cells Respond Functionally to Acoustic Stimuli in the Awake Monkey Brain

Graphical Abstract

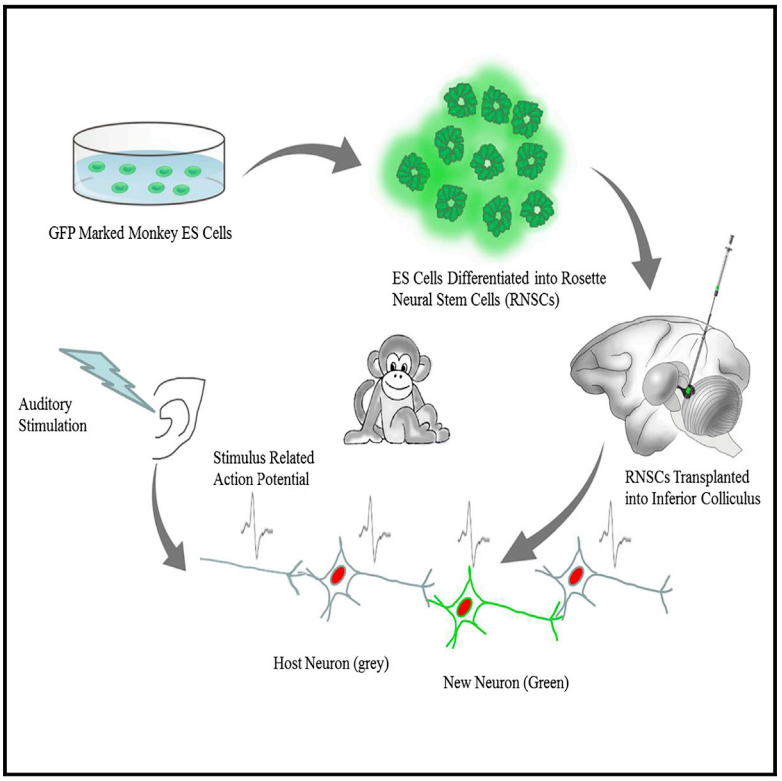

Highlights

- Stem cells were transplanted into the inferior colliculus (IC) of rhesus monkeys
- Differentiated neurons formed reciprocal anatomical connections with host neurons
- Some differentiated neurons responded to auditory stimuli in an IC-specific manner
- Transplanted stem cells likely integrated into host neural networks

Authors

Jing-kuan Wei, Wen-chao Wang, Rong-wei Zhai, ..., Dong-dong Qin, Xin-tian Hu, Zheng-bo Wang

Correspondence

xthu@mail.kiz.ac.cn (X.-t.H.), wangzb@mail.kiz.ac.cn (Z.-b.W.)

In Brief

Integration of differentiated neurons into a functioning neural network is important for the development of stem cell therapies. Wang et al. found that neurons differentiated from transplanted stem cells respond to auditory stimuli in awake monkeys after transplantation.

Wei et al., 2016, Cell Reports *16*, 1016–1025
July 26, 2016
http://dx.doi.org/10.1016/j.celrep.2016.06.066

OPEN ACCESS
CellPress

Cell Reports
Article

Neurons Differentiated from Transplanted Stem Cells Respond Functionally to Acoustic Stimuli in the Awake Monkey Brain

Jing-kuan Wei,[1,6,7] Wen-chao Wang,[1,6,7] Rong-wei Zhai,[1,6,7] Yu-hua Zhang,[1] Shang-chuan Yang,[1] Joshua Rizak,[1] Ling Li,[3] Li-qi Xu,[3] Li Liu,[3] Ming-ke Pan,[1] Ying-zhou Hu,[1] Abdelaziz Ghanemi,[1] Jing Wu,[1] Li-chuan Yang,[1] Hao Li,[1] Long-bao Lv,[4] Jia-li Li,[1] Yong-gang Yao,[1,2] Lin Xu,[1,2] Xiao-li Feng,[1] Yong Yin,[5] Dong-dong Qin,[1] Xin-tian Hu,[1,2,4,*] and Zheng-bo Wang[1,*]

[1]Key Laboratory of Animal Models and Human Disease Mechanisms of Chinese Academy of Sciences and Yunnan Province, Kunming Institute of Zoology, Kunming, Yunnan 650223, China
[2]CAS Center for Excellence in Brain Science and Intelligence Technology, Chinese Academy of Sciences, Shanghai 200031, China
[3]Medical Imaging Department, Kunming General Hospital of PLA, Kunming, Yunnan 650032, China
[4]Kunming Primate Research Center, Kunming Institute of Zoology, Chinese Academy of Sciences, Kunming, Yunnan 650223, China
[5]Department of Rehabilitation Medicine, Fourth Affiliated Hospital of Kunming Medical University, Kunming, Yunnan 650021, China
[6]Kunming College of Life Science, University of Chinese Academy of Sciences, Kunming, Yunnan, 650204, China
[7]Co-first author
*Correspondence: xthu@mail.kiz.ac.cn (X.-t.H.), wangzb@mail.kiz.ac.cn (Z.-b.W.)
http://dx.doi.org/10.1016/j.celrep.2016.06.066

SUMMARY

Here, we examine whether neurons differentiated from transplanted stem cells can integrate into the host neural network and function in awake animals, a goal of transplanted stem cell therapy in the brain. We have developed a technique in which a small "hole" is created in the inferior colliculus (IC) of rhesus monkeys, then stem cells are transplanted in situ to allow for investigation of their integration into the auditory neural network. We found that some transplanted cells differentiated into mature neurons and formed synaptic input/output connections with the host neurons. In addition, c-Fos expression increased significantly in the cells after acoustic stimulation, and multichannel recordings indicated IC specific tuning activities in response to auditory stimulation. These results suggest that the transplanted cells have the potential to functionally integrate into the host neural network.

INTRODUCTION

Neural stem cell (NSC) transplantation has been demonstrated to facilitate the recovery of functional loss resulting from neurodegenerative diseases (Rossi and Cattaneo, 2002) and/or brain/spinal cord injury (Sahni and Kessler, 2010; Thuret et al., 2006). This suggests that NSCs have therapeutic potential for such impairment, although the mechanism underlying the observed recovery is controversial. A number of researchers have attributed this recovery to the secretion of trophic factors or their derivatives by the transplanted NSCs. The trophic factors then slow or prevent the deterioration of the degenerating neurons (Blurton-Jones et al., 2009; Breunig et al., 2011; Lu et al., 2003). Alternatively, others have suggested that the neurons differentiated from the transplanted NSCs might substitute for the injured or lost neurons by functionally integrating into the host neural circuitry (Englund et al., 2002; van Praag et al., 2002; Weick et al., 2011).

Although both possibilities have potential benefits for treatment, the functional integration of transplanted NSCs into the host neural network is a cornerstone for the future of NSC clinical applications. This study was developed to examine whether transplanted NSCs can function in an awake animal brain. Here, a "cut-and-fill" technique that confines the transplanted NSCs to a small cylindrical space in rhesus monkey brain was developed (as outlined in Experimental Procedures), allowing the use of immunohistochemical and neuro-electrophysiological techniques to investigate the integration of stem-cell-derived neurons in awake animals.

The inferior colliculus (IC) was selected as the site of transplantation, since almost all IC neurons show strong responses to auditory stimuli at a wide range of intensities and frequencies (McAlpine et al., 2001; Schnupp and King, 1997). Moreover, the deep location of the IC within the brain provides a number of advantages to other brain areas, such as the primary visual cortex (V1) or the primary somatosensory cortex (S1), because it minimizes the effects of natural brain shifting and pulsations on the electrophysiological recording as well as having a higher firing rate in response to stimuli. A high firing rate in the transplant area increases the possibility of establishing new connections between the host and transplanted neurons in accordance with Hebb's law: neurons that fire together, wire together (Hebb, 1949).

RESULTS

"Cut-and-Fill" Transplantation Strategy

Post-mortem immunohistological examination of the surgery site demonstrated that the "cut-and-fill" strategy created a

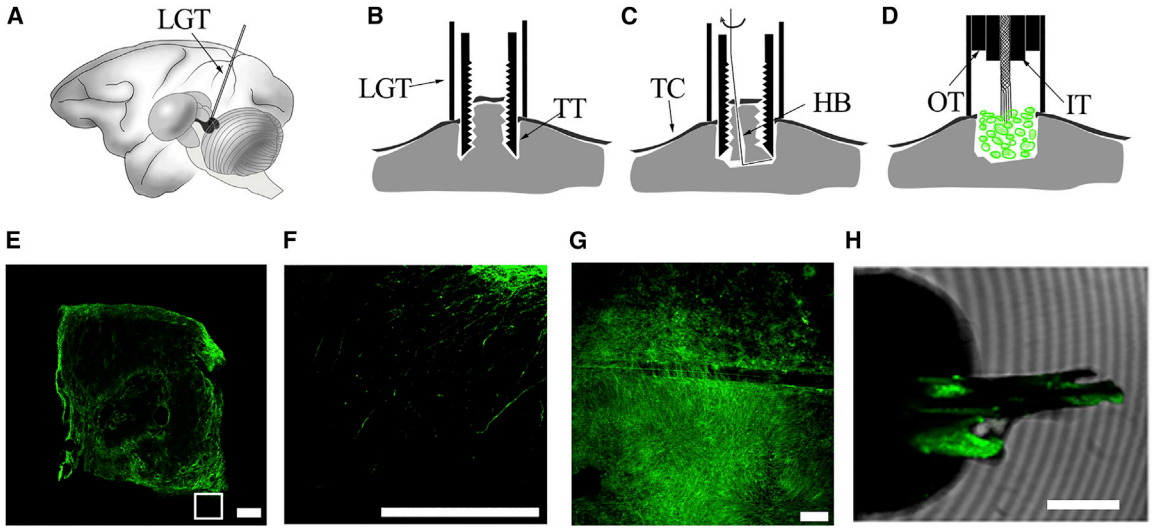

Figure 1. Schematic Diagrams Showing the Mechanical Lesion Procedure of Developing the IC Transplantation Model and GFP-Labeled Transplanted NSCs' Histological Images

(A) A localization guide tube (LGT) was inserted into the brain until it came into contact with the IC (black).

(B) A thin tube with internal threads and a sharp-toothed tip was used to make an incision on the dura membrane and to separate part of the IC tissue. TT, thin tube with internal threads and a sharp-toothed tip.

(C) A hook-shaped needle blade separated the bottom IC tissue to form a "hole." HB, hook-shaped needle blade; TC, tentorium cerebelli.

(D) A cross-section shows the transplantation of GFP-labeled NSCs and the placement of the single-unit recording electrode. IT, inner tube; OT, outer tube.

(E) A histological image showing the survival of GFP-labeled cells transplanted into a "hole" in the IC. The transplanted GFP-labeled cells have a clear boundary with the host IC tissue.

(F) A detailed view of the inset in (E) shows the projections of the transplanted NSCs into the surrounding host tissue.

(G) GFP-labeled NSCs grown in the presence of electrode for 7 days.

(H) An image of transplanted GFP-labeled cells attached to an electrode removed from a monkey IC.

Scale bars, 250 μm in (E) and (F), 50 μm in (G), and 60 μm in (H).

cylindrical "hole" with a well-defined boundary between the surrounding brain tissue in the IC and the transplanted cell mass (Figure 1E; Figure S1; Table S1). The transplanted NSCs generated a large number of fibers projecting into the surrounding brain tissue (Figure 1F; discussed later). Furthermore, the recording electrode used in this study had a good biocompatibility for at least 6 months, as indicated by the survival of many GFP-labeled cells attached to the recording electrode after its removal from the transplantation site (Figure 1H).

Transplanted NSCs Survived and Differentiated into Mature Neurons

Further immunohistochemical experiments were conducted 6 months after the transplantation to determine whether the surviving transplanted NSCs had differentiated into neurons. The cells were evaluated for classic neural markers: NeuN, Tau, and Map2 (Figures 2A–2C). Transplanted GFP+ cells were stained with NeuN/Tau or NeuN/Map2. The cells were found to have a clear formation of the nucleus and cytoskeleton, indicating differentiation into mature neurons (Figures 2A and 2B) with notable axonal projections (Figure 2C). Approximately 12.2% of the surviving transplanted NSCs had differentiated into neurons (Figures 2D and 2J), while about 29.4% of cells around the area of transplantation were found to be NeuN positive in host IC tissues (Figure 2J).

The area of transplantation was also stained with dendritic and synaptic markers to determine whether the transplanted NSCs formed neuronal connections with host neurons. Map2 staining at the edge of the transplanted site showed that there were abundant dendritic fibers sprouting into the surrounding host brain tissue (Figure 2E). Synapsin I, a major phosphoprotein found on synaptic vesicles (Ferreira and Rapoport, 2002; Rosahl et al., 1993) and a classic presynaptic membrane marker, was used to identify presynaptic terminals. Some presynaptic terminals from host neurons (Synapsin I positive, GFP negative) were identified inside the transplanted tissue (Figure 2F). These results, taken together with PSD-95 (postsynaptic density protein-95; Hunt et al., 1996)-positive staining (Figure 2I), showed that a large number of synapses originating from host neurons formed on the differentiated neurons in the site of transplantation. These synapses might provide the anatomical foundations for the host neurons to send neuronal signal outputs to the differentiated neurons.

These data also demonstrated that projections from the differentiated neurons to the host neurons were formed (Figures 2G and 2H). For example, the axons of some of the differentiated neurons (GFP-positive cells co-labeled with Tau) projected into the host tissue and sprouted around the host neurons (Figure 2G). Moreover, some presynaptic terminals from the differentiated neurons (GFP-positive cells co-labeled with Synapsin I) were identified in the host tissue (Figure 2H).

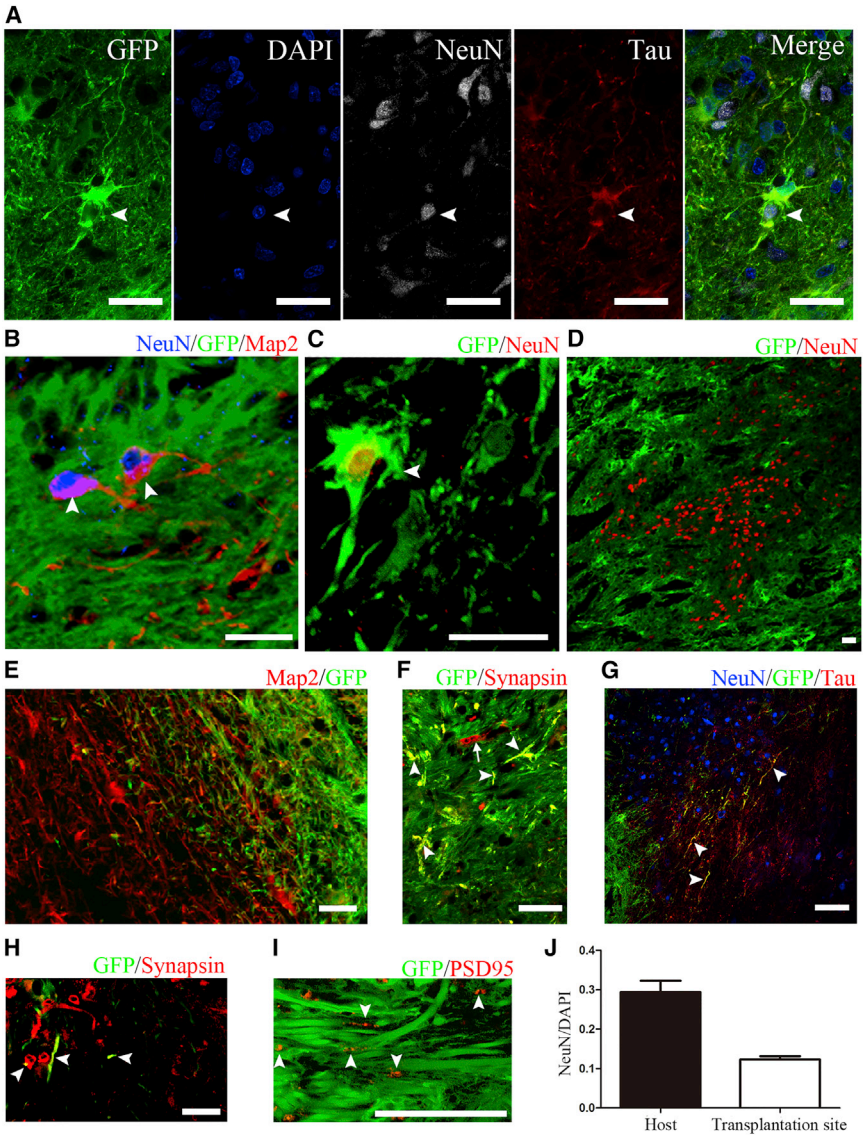

Figure 2. Transplanted NSCs Differentiated into Mature Neurons and Formed Synapses with Neighbor and Host Neurons

(A) A transplanted NSC (GFP) differentiated into a mature neuron (arrowhead; neuronal nucleus, NeuN, white; axons and other neurites, Tau, red).

(B) Two mature neurons differentiated from transplanted NSCs (arrowheads) (NeuN, blue; dentritics, Map2, red).

(C) A differentiated neuron (arrowhead) with a clear axon (NeuN, red; GFP, green).

(D) At lower magnification, a large number of transplanted NSCs differentiated into neurons (NeuN, red).

(E) The border of the transplant site. Dendritic fibers of engrafted NSCs sprouted into the host brain (Map2, red).

(F) Host (arrow) and the differentiated neuron (arrowheads) presynaptic terminals in the transplanted tissue (Synapsin I, red).

(G) Axons (arrowheads; Tau, red) of the differentiated neurons (GFP) projected around host neurons (NeuN, blue).

(H) Differentiated neurons formed presynaptic terminals (arrowheads; synapsin I, red) in the host IC.

(I) Postsynaptic terminals (arrowheads) of the differentiated neurons (PSD-95, red).

(J) The ratios of neurons (NeuN labeled) to all cells (DAPI labeled) in area of transplantation and the host IC tissues around the area in an area of 0.4 mm^2. About 12.2% of transplanted cells differentiated into neurons (n = 31), and approximately 29.4% of cells were neurons in host IC tissues around the area of transplantation (n = 17). Error bars indicate SEM. Scale bars, 30 μm. See also Table S5.

All told, these immunohistochemical data demonstrated that the NSCs survived after the transplantation, that the cells differentiated into mature neurons, and that synaptic structures were formed between the differentiated neurons and host neurons. This suggests that an anatomical and cellular basis for neuronal signals to flow into and out of the transplanted area was established.

Sound-Evoked c-Fos Expression Marks Activity of the Neurons Differentiated from the Transplanted NSCs

c-Fos, an immediate early gene and proto-oncogene, is highly expressed in active cells (Gutman and Wasylyk, 1991) and has been used as an effective tool to investigate cellular activity in the brain because the number of c-*fos*-positive neurons in an activated brain region continuously and significantly increases for 2 hr following a stimulus (Miyata et al., 2001). The monkeys in this study were given auditory stimulation to induce auditory responses from the differentiated neurons in the IC, and c-*fos* expression was used to demonstrate the activities. Five awake monkeys were divided into two groups and put individually into an anechoic chamber. The first group consisted of three monkeys that had been kept in the chamber without sound stimulation for 2 hr followed by exposure to a wide band white-noise stimulus (80 dB) for 30 min. After which, the monkeys were kept in the chamber without stimulation for another 90 min. The other two monkeys (control group) were put in the same chamber without any sound stimulus for 4 hr. After the respective 4-hour periods, each animal was immediately sacrificed, and the brain tissues were fixed in 4% paraformaldehyde.

The expression of c-Fos protein in the differentiated neurons after the stimulus was identified with the co-expression of NeuN (Figures 3A and 3B). Although c-*fos* was expressed in the differentiated neurons of all five monkeys, the control group (without sound stimulus) had a significantly lower expression level in the area of transplantation than the monkeys of the sound stimulus group ($p < 0.01$) (Figure 3C). Most of the differentiated neurons in the stimulated group were c-*fos* positive (about

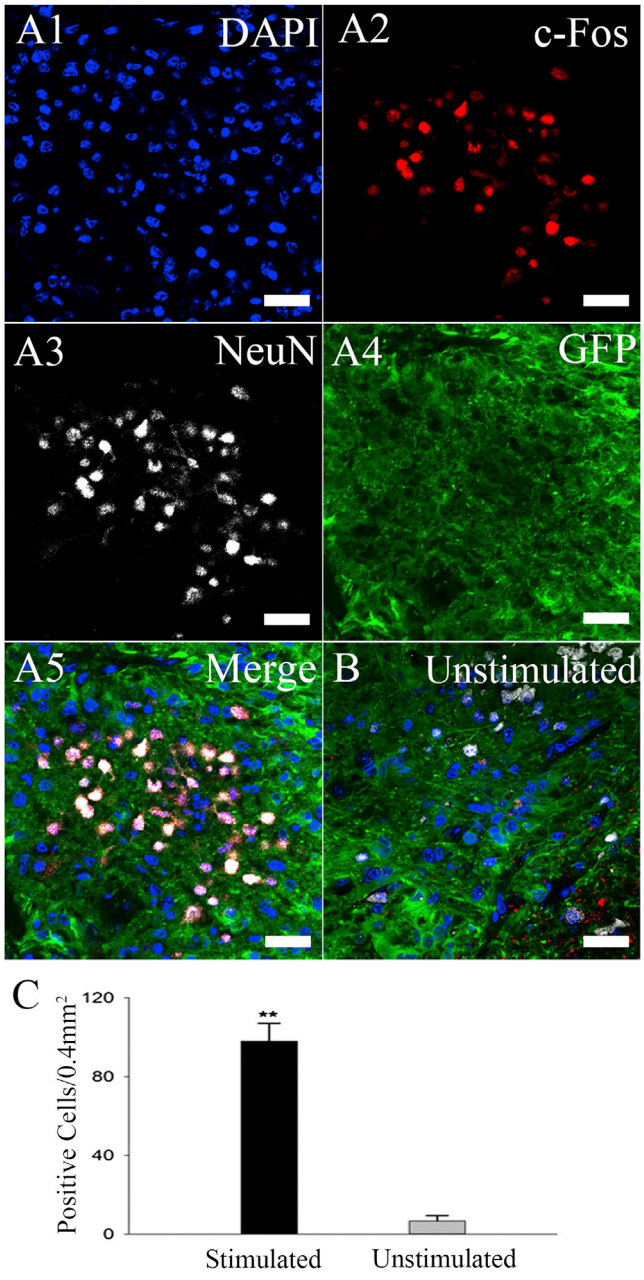

Figure 3. Comparison of c-*fos* Expression in the Differentiated Neurons in Acoustically Stimulated Monkeys and Non-stimulated Monkeys

(A) Co-labeling (NeuN/c-*fos*) of the differentiated neurons in the auditorily stimulated group (n = 3) showed high activity (arrows). A1 displays all cell nuclei stained by DAPI (blue). A2 displays active cells responding to stimulus stained by c-*fos* (red). A3 displays neuronal nuclei staining (NeuN, white). A4 displays surviving transplanted cells (GFP, green). A5 displays the merged image.

(B) Active differentiated neurons (arrow) in the non-auditorily stimulated group (n = 2) were visualized by co-labeling with NeuN (white) and c-*fos* (red).

(C) c-Fos expression in the auditorily stimulated group was significantly higher than in the non-stimulated group. **$p < 0.01$.

Error bars represent SEM. Scale bars, 30 μm. See also Table S5.

70% of the differentiated neurons were activated, i.e., GFP-positive cells co-labeled with NeuN and c-*fos*; Figures 3A1–3A5). These findings demonstrated that there were robust auditory neuronal activities among the differentiated neurons (Figure S1). This suggested that the differentiated neurons had received stimulus-evoked neuronal inputs from host IC neurons through the synaptic connections demonstrated in the immunohistochemical experiments discussed earlier. These findings suggest that, after processing these inputs, the differentiated neurons generated action potentials and then likely sent them out to host neurons in the IC through projections between them (for additional evidence, please refer to the single-neuron recording study section) and that the differentiated neurons may function in the awake animal brain.

Electrophysiological Recording from the Transplanted Area after Acute Auditory Stimulation

While the c-*fos* expression demonstrated that a substantial number of the differentiated neurons showed auditory stimulation related activities, a multi-single-neuron recording technique was used in situ to get a better observation of the firing characteristics of the differentiated neurons. The recordings were conducted in the site of transplantation of five awake monkeys after the animals were given 2 weeks to recover from the NSC transplantation surgery. Single-neuron activities were recorded under auditory stimulation for a time period of 18 to 22 weeks.

During the first 3 to 4 weeks of the recording period, no neuronal discharges were detected. From the fourth week onward, spontaneous spike signals were recorded in the upper part of the transplanted tissue in five monkeys. The electrode was not driven down further into the transplanted mass until spontaneous activity had been observed in the IC. This time course is consistent with previously reported time frames for engrafted stem cells to differentiate into functional neurons (Southwell et al., 2014). This suggests that the first 6 weeks after transplantation might be an important time period for the transplanted NSCs to differentiate into mature neurons.

After the fourth week, up to the 22nd week, the electrode was gradually moved down to record from the differentiated neurons. By the end of the recording period, a total of 19 neurons were recorded in the five awake monkeys (Table S2). Five of these 19 neurons showed clear responses to the auditory stimuli. Typical responses of three neurons are shown in Figure 4B. The waveforms of the spikes were similar to the characteristics of a typical cell-body spike's waveform rather than those of an axon's waveform (Figures 4C, 5A, and 5J) (Fuortes et al., 1957; Humphrey and Schmidt, 1990). Each waveform had an obvious hyperpolarization and lasted for a duration of 1 ms. This characteristic was observed from all 19 neurons. The spikes of a representative neuron (m07403-3; Figures 4C and 4D) in response to pure tones of 8000 Hz and 95 dB was tightly correlated to the onset and offset of the auditory stimulation and had a latency around 15 ms, This latency is similar to the normal latency of IC neurons reported by Ryan and Miller (1978). This suggests that neuron m07403-3 received functional excitatory inputs from host neurons and integrated them before generating action potentials.

Previous studies have shown that one of the responsive characteristics of the IC neuron is that it responds optimally to a

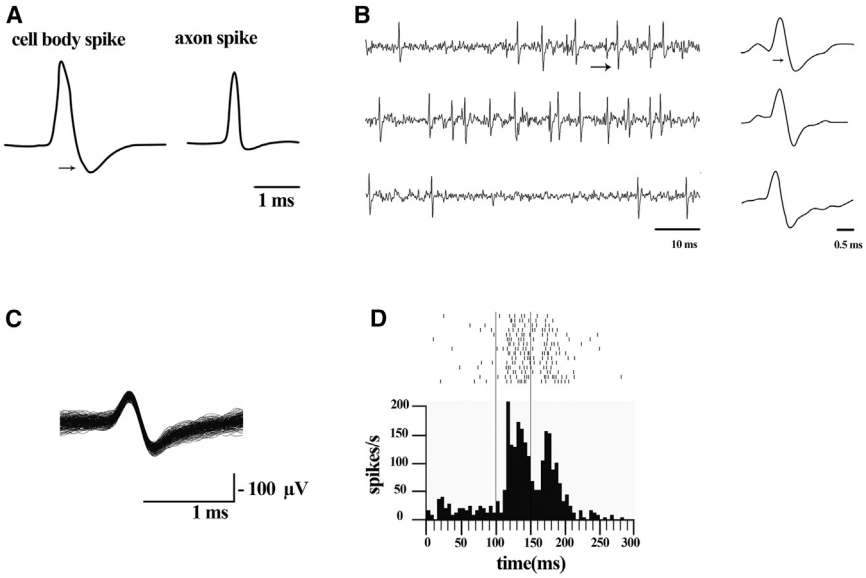

Figure 4. The Differentiated Neurons Have Typical Action Potential Waveforms of a Cell-Body Spike and Similar Auditory-Stimulus-Related Responses to Host IC Neurons

(A) Typical cell-body and axon spike voltage waveforms. The cell-body spike has an obvious hyperpolarization (arrow) and a duration of 1 ms, whereas the axon spike lacks the hyperpolarization component in the waveform and has a shorter duration (about 0.5 to 0.7 ms).

(B) Spike trains from three different somas of the differentiated neurons. They all had a clear hyperpolarization phase (arrows) and lasted for a duration of 1 ms.

(C) The voltage waveforms recorded from a differentiated neuron (m07403-3) when the monkey was stimulated with an auditory stimulus of 8000 Hz and 95 dB.

(D) A raster plot and histogram show an atypical time-locked differentiated neuron's response (15 ms in latency) to an auditory stimulus (the vertical lines on the histogram at 100 ms and 150 ms indicate the onset and the offset of the stimulus, respectively). The spikes appeared tightly correlated to the onsets and offsets of the auditory stimulation with a latency around 15 ms, which is similar to the normal latency of a host IC neuron.

specific frequency (an optimum frequency) (Zwiers et al., 2004). To determine the individual optimum frequency of five differentiated neurons that displayed clear responses to the auditory stimuli, the auditory responses of the five neurons were further tested, with pure tones at different frequencies ranging from 200 Hz to 10000 Hz at an intensity of 80 dB. The recordings from neuron m09311-3 (located less than 1 mm under the IC surface; Figure 5B) showed that it had a typical responsive frequency area and its optimal frequency was 2,000 Hz (Figures 5C–5I). This activity is similar to previously reported data recorded from neurons located 1 mm under the IC subsurface (Zwiers et al., 2004). This suggests that neuron m09311-3 did not randomly respond to the stimuli and had acquired certain local properties of the IC, especially in terms of stimulus frequency selectivity.

In addition to frequency tests, the differentiated neurons were also examined for how they responded to changes in sound intensity. In the experiments, the monkeys were exposed to white noise with different intensities (60, 65, 70, 75, 80, 85, 90, and 95 dB). Three neurons were found to be monotonic to the sound intensity changes, and the responses from a representative neuron (m09311-4) are shown in Figures 5K–5S. This indicated that their firing rates increased with the increment of sound intensity. This property has been reported as a typical feature of IC neurons (Zwiers et al., 2004).

Among the 19 neurons recorded from the five monkeys, five neurons showed frequency/intensity-related activities (Figure 5; Table S2). Among these five neurons, two changed their firing rates as the frequency varied, two responded monotonically to sound intensity increases, and one showed response changes to both. These results indicated that these differentiated neurons had a coding feature tuning to the external stimuli and demonstrated similar firing characteristics to previously reported IC neurons.

Another common responsive property of the IC neuron is that its responses will decline with the repetition of same auditory stimuli. This feature is a result of an adaptation of either the neuron itself or the whole neural network (Borisyuk et al., 2002). This adaptive property was observed in two differentiated neurons, which had received 60 identical auditory stimuli (The average intertrial interval [ITI] was 2 s, and each stimulus lasted for 200 ms; Figure 6). The data from a representative neuron (m09311-5) are shown in Figure 6. Its firing rate was above 20 spikes per second for the first block of 20 identical stimulations. The discharge rate decreased to approximately 17 spikes per second for the second block of 20 stimulations. For the last block of 20 stimulations, the firing rate dropped to around six spikes per second (Figure 6). These data indicated that these two differentiated neurons displayed an adaptive response property similar to that of previously reported IC neurons (Borisyuk et al., 2002).

All told, the single-neuron recording data from the site of transplantation provided details regarding the activity characteristics of the differentiated neurons. Specifically, some of the differentiated neurons exhibited tuning activities, such as tuning to frequency/intensity changes, and adapted to the repetition of auditory stimuli. These properties are similar to reported properties of IC neurons and suggest that the differentiated neurons may function in awake animals.

DISCUSSION

In this study, stem cells were transplanted into a small "hole" introduced into the IC of rhesus monkeys in order to evaluate the integration of the differentiated neurons into the host neural network. Immunohistochemical data demonstrated that the transplanted NSCs differentiated into mature neurons and formed input/output synaptic connections with host neurons.

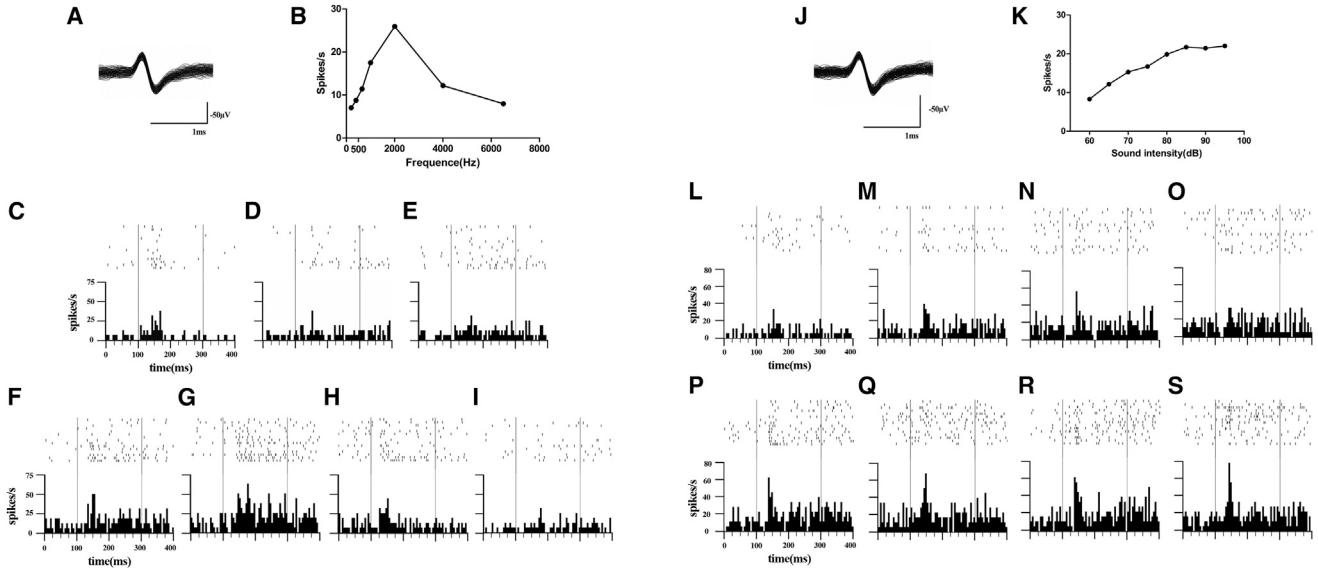

Figure 5. Responses of Differentiated Neurons to the Frequency and Intensity of Auditory Stimuli in Awake Monkeys

(A) Voltage waveforms recorded from a representative neuron (m09311-3) when the animal was stimulated with an optimized sound stimulus (2000 Hz). The waveforms have the hyperpolarization and long duration of a soma spike.

(B) Frequency response area of neuron m09311-3.The firing rates in the chart are calculated from the data in (C)–(I).

(C–I) Raster plots and histograms reveal the responses from neuron m09311-3 to pure-tone stimuli with different frequencies at an intensity of 80 dB: the responses were to frequencies at 200, 400, 650, 1000, 2000, 4000 and 6500 Hz, respectively.

(J) Voltage waveforms of a representative neuron (m9311-4) when the animal was stimulated with white noise at an intensity of 75 dB.

(K) The firing rate level function of neuron m09311-4 (white noise). The firing rates are calculated from the data in (L)–(S).

(L–S) Raster plots and histograms reveal the responses of neuron m09311-4 to white-noise stimuli with different sound levels: 60, 65, 70, 75, 80, 85, 90, and 95 dB.

This indicated that the transplanted NSCs had integrated into the host neural network. c-Fos expression was used to study the regional response of the differentiated neurons to auditory stimulation. Around 70% of the differentiated neurons showed increased c-*fos* expression after receiving auditory stimulation. This indicated that the differentiated neurons received stimulus-evoked neuronal inputs from host IC neurons. After integrating the inputs on their cell bodies, those differentiated neurons generated action potentials that, in turn, likely sent out spikes to the host neurons. In addition, a multi-channel single-neuron recording technique was used to record and illustrate neuronal activity in the site of transplantation. The recordings showed that some of the differentiated neurons displayed tuning activities similar to previously reported activities of IC neurons (Borisyuk et al., 2002; Zwiers et al., 2004). This indicated that the differentiated neurons received excitatory inputs and processed them in order to exhibit IC-specific tuning activities and responses. All of these findings suggest that the transplanted NSCs have the potential to integrate into the host neural network and function in the awake animal brain.

Previous research on the integration of neurons differentiated from stem cells into host networks has been carried out predominantly on brain slices. This research has found that engrafted embryonic stem cell (ESC)-derived neurons formed synaptical connections with host neurons and received artificially induced excitatory and inhibitory synaptic inputs from host neurons, such as electrical, glutamatergic, or GABA stimulation of the host tissue (Benninger et al., 2003; Englund et al., 2002; Wernig et al., 2004; Zhou et al., 2015). In another study performed on acute mouse brain slices, transplanted neurons differentiated from human ESCs expressing channelrhodopsin-2 were found to elicit both inhibitory and excitatory postsynaptic currents after optical stimulation and to produce postsynaptic signals in host pyramidal neurons (Weick et al., 2011). Moreover, previous reports have demonstrated that new neurons generated during adult neurogenesis in the mouse hippocampus display passive membrane properties and action potentials under current clamp on live slices (van Praag et al., 2002). These results suggested that new neurons—and, in particular, neurons differentiated from stem cells—are capable of integrating into the brain circuitry through the formation of new synapses. However, these results did not confirm functional neuronal activity and integration of the transplanted NSCs in awake animal brains.

To examinate whether transplanted NSCs can integrate into the host neural network and function in awake animals, we developed a "cut-and-fill" transplantation strategy to directly study the behavior and function of the transplanted NSCs in rhesus monkey brains. This strategy had a number of advantages over previous studies performed in brain slice investigations. This strategy utilized a brain region localization technique to target the IC with pinpoint accuracy, a mechanism to create a well-controlled and accurate lesion of the IC tissue and an effective measure to prevent the drifting or migration of the transplanted NSCs. In addition to these measures, the strategy accurately placed a multi-channel recording electrode within the transplant mass in order to directly investigate the functional integration of

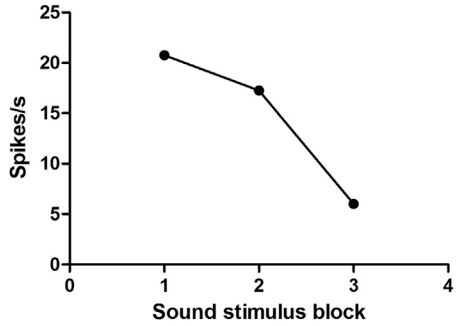

Figure 6. Adaptive Property of a Differentiated Neuron
A line chart demonstrates a decrease of firing rates of a representative neuron (m09311-5) when the monkey was stimulated by a repeated identical-sound stimulus.

the transplanted NSCs in response to specific stimuli in awake animal brains. Using this strategy, the cells were found to form anatomical connections with host neurons, to be activated by auditory stimuli, and to respond to stimuli in an IC-specific manner. This suggests that transplanted stem cells have the potential to integrate into the host neural network and function in awake animals.

Single-neuron recording was used to provide some examples and illustrate the details of firing pattern of the differentiated neurons within the transplant area. We recorded auditory responses from 19 of the neurons and found that five of them responded to the auditory stimuli in a manner similar to that of previously reported IC neurons (Borisyuk et al., 2002; Zwiers et al., 2004). The relatively low number of recorded neurons identified was partially a result of the recording being conducted within transplanted tissue, whose physiological environment and neuronal population were much different from normal brain tissue. It also should be noted that the 19 neurons had been recorded for a time period of 18 to 22 weeks. This time frame is thought to be a period when the transplanted NSCs gradually mature and integrate functionally into the host neural network. In addition, the recording electrodes had limited movement during the single-neuron recording period (as mentioned in Results), which may have also contributed to the low neuron number recorded in the area of transplantation. Nonetheless, the auditory-responsive data recorded from the five neurons that displayed IC-specific tuning properties illustrates the physiological development of synaptic connectivity and some details of the firing patterns of the neurons within the area of transplantation. Future experimentation is required to evaluate the overall auditory processing properties of the whole area of transplantation in order to gauge the full potential of the transplanted NSCs to integrate into the host neural network and function in awake animals.

While it is preliminary to fully assess the ability of transplanted stem cells to differentiate and replace lost neurons in a damaged brain, the present findings provide impetus for further, yet more sophisticated, experimentation to be conducted in order to address these important and difficult issues. This study used a "cut-and-fill" technique to investigate the functional responses of the transplanted NSCs in awake animal brains and provides a strong foundation to evaluate the full functional integration of transplanted stem cells in the future. More importantly, this study provides encouragement that further optimization of neuronal differentiation from stem cells may make stem cell replacement therapy in the brain and nervous system a reality in the not-too-distant future.

EXPERIMENTAL PROCEDURES

LYON-ESC Culture

GFP-marked rhesus monkey ESCs (a gift from the Lyon Stem Cell Research Institute; Wianny et al., 2008) were cultured in ES medium containing Knockout (KO)-DMEM (Invitrogen), 20% KO-SR (KO serum replacement) (Invitrogen), 1% nonessential amino acids (Invitrogen), 2 mM L-glutamine (Sigma-Aldrich), 0.1 mM β-mercaptoethanol (Sigma-Aldrich), and 10 ng/ml basic fibroblast growth factor (bFGF) (Invitrogen). The medium was changed every day, and mechanical passaging of undifferentiated colonies was performed manually every 5–7 days by cutting the colonies into large clumps using a flame-pulled Pasteur pipette. The LYON-ES Cs were co-cultured with mitotically inactivated mouse embryonic fibroblasts (CF-1-MEFs; ATCC). The CF-1-MEFs were first grown in DMEM (Invitrogen) with 2 mM L-glutamine supplemented with 15% FBS (Invitrogen). All cells were grown at 37°C in 5% CO_2.

NSC Induction

In order to induce NSCs, LYON-ESC colonies were digested with 1 mg/ml dispase, washed with ES medium to remove the dispase, and suspended in modified N/M medium (Pankratz et al., 2007), which contained 50% DMEM/F12 (Invitrogen), 50% neural basal medium (Invitrogen), 1 × N2 supplement (Invitrogen), 1 × B27 (Invitrogen), and 2 mM L-glutamine. Then, the cells were plated in a 15 mm × 30 mm well coated with agar (Sigma-Aldrich). The cells were allowed to aggregate for 4 days to form embryonic bodies (EBs). After this aggregation, EBs were selected and cultured in NP media in four-well plates coated with extracellular matrix (ECM; Sigma-Aldrich) for 10 to 14 days till rosette formation appeared. The NP media contained DMEM/F12, 1 × ITS-x (Invitrogen), 2 ng/ml heparin (Sigma-Aldrich), and 2 mM L-glutamine.

Neural rosette cell aggregations were then dissociated into small cell clumps by gentle pipetting. The cell suspensions were sampled and treated with trypsin (0.05% in 0.1% EDTA) for cell counting. Then, the neural rosette cells were suspended in PBS at a concentration of 10^7 cells per microliter and placed on ice for transplantation.

Monkey Fibroblast Cell Culture

Rhesus monkey fibroblasts were cultured in DMEM, containing 15% FBS and 0.1% streptomycin and gentamycin (Sigma-Aldrich) at 37°C in 5% CO_2. The cell cultures were collected and treated with trypsin (0.05% in 0.1% EDTA) for cell counting. Cells were suspended in PBS at a concentration of 10^7 cells per microliter and placed on ice for transplantation.

Immunocytochemistry of NSCs

After selection of rosette-forming cells and prior to transplantation into each monkey, a small portion of the selected cells was stained with Nestin/Tuj/Map2/Sox1/Oct4 to examine the purity of the neural progenitor population (Figure S2). The results showed that the purity of NSCs was very high and that no undifferentiated ESCs or differentiated neurons were evident. Since the ESCs and neurons were very scarce in the tests, no other NSC purifying procedure was used, except hand picking of the rosette cells. As a second confirmation, some of the grafted cells were kept to be stained after transplantation with Nestin/Tuj/Map2/Sox1/Oct4. The results were similar to the previous purity tests.

Cells for the NSC immunocytochemistry test were cultured on chamber slides and fixed in 4% paraformaldehyde (Sigma-Aldrich) in PBS for 20 min and then permeabilized with 0.1% Triton X-100 (Sigma-Aldrich) for 15 min. The slides were then blocked for 1 hr at room temperature in PBS containing 5% BSA (Sigma-Aldrich). Samples were then incubated in blocking buffer (1% BSA) containing primary antibody overnight at 4°C. Following three 5-min washings with PBS, cells were then incubated with secondary antibodies conjugated with Texas Red (1:200, Sigma-Aldrich) for 2 hr at 37°C. The samples

were washed using the same procedure as mentioned earlier and mounted with DAPI (Dako) containing mounting solution.

The following primary antibodies were used: Tubulin Beta III, Nestin, Map2, Sox1, and Oct4. Fluorescent samples were examined with a FV1000 fluorescence microscope (Olympus). The information of primary and secondary antibodies is presented, respectively, in Tables S3 and S4.

Biocompatibility Test of Polyimide-Film-Coated Electrodes with Cultured Monkey NSCs

Five platinum-iridium wires (2 mm in length, 25 μm in diameter) were placed in a dish where the rosette-shaped NSCs were cultured. Results showed that the wires exerted no significant cytotoxicity on the cells. The cells had adhered to the surface of the wire electrodes, and no obvious deformation of the attached cells was observed (Figure 1G). This suggested that the growth and proliferation of the cultured cells was not affected by the polyimide-film-coated wire electrodes.

"Cut-and-Fill" Transplantation Strategy: IC Lesion Surgery, NSC Transplantation, and Electrode Implantation

Seven (two of fibroblast control) rhesus monkeys (*Macaca mulatta*, 4–6 years old, weighing 6.5–7.5 kg) were used in this study. The monkeys were purchased from the breeding colonies of Kunming Primate Research Center, Kunming Institute of Zoology, Chinese Academy of Sciences.

All animal procedures conformed to the requirements of the Animal Welfare Act (People's Republic of China) and were approved by the Institutional Animal Care and Use Committee (IACUC) of the Kunming Institute Zoology, Chinese Academy of Sciences (Approval ID: SMKX-2016014).

An MRI-guided location technique with an accuracy of 0.5 mm developed previously in our lab (Jing et al., 2010) was used for each monkey to accurately locate the IC, a small nucleus deep in the monkey midbrain. After being anesthetized with hydrochloric acidulated ketamine (10 mg/kg, intramuscularly [i.m.]) and maintained with sodium pentobarbital (20 mg/kg, i.m.), each monkey's head was mounted on a stereotaxic apparatus (Shenzhen Reward Life Science). Three MRI-visible external markers (three rigid glass tubes, with 0.5 mm internal diameters, filled with a vitamin AD solution that is visible in the MRI) were anchored on each monkey's skull with dental acrylic. The surgery to attach the external MRI markers and specific MRI parameters has been outlined in detail previously (Jing et al., 2010). Of note, the orientation of the MRI images was set to correspond to the monkey's head within the stereotaxic frame by adjusting the scanning angle to scan through the plane of two of the three markers, which were placed on the calvarial sagittal suture, during the MRI capture. The third marker was placed near the IC location, as estimated according to an anatomical atlas of rhesus monkey brain. The relative coordinates of the IC in relation to the three external markers were later determined from MRI images of each monkey (Figure S3A).

Based on the relative IC coordinates obtained from the MRI, a localization guide tube (LGT) with an inner diameter of 1.5 mm was inserted into the monkey's brain obliquely, making it perpendicular to the IC surface. Then, a thin probe was inserted into the brain through the LGT to measure the depth of the targeted IC surface from the skull. This approach was based on a technique developed previously in our lab to pierce the tentorium cerebelli (TC) covering the IC (Wu et al., 2014). When the probe reached the surface of the IC, it recoiled due to the surface tension of the dura matter, thereby confirming the depth of the IC surface from the skull of each individual monkey. Then, the LGT was driven down to this measured depth and anchored onto the skull with dental cement. This precise placement of the LGT helped to accurately locate the lesion site on the IC (Figures S3B, S3C, S3E, and S4B). Then a mechanical separator was used to make a lesion into the IC. The separator consisted of a hook-shaped needle blade and a thin tube with an internal thread and a sharp-toothed tip. The thin tube was 2 mm longer than the LGT. First, the thin tube was gently put into the LGT until it reached the TC. By rotating the thin tube, its sharp-toothed tip cut off the TC and went down to its final depth (2 mm longer than the LGT) (Figure 1B). Then, a hook-shaped needle blade was inserted into the thin tube, and the IC tissue within the tube was cut off and removed by rotating the needle blade (Figure 1C). After this mechanical "cut" operation, a cylindrical "hole" (1.5 mm in diameter; about 2 mm in depth) in the IC was created. To prevent changes in both the size and shape of the "hole," a stainless steel plug (2 mm longer than the LGT) was inserted to fill the "hole."

When the environment in the hole was optimum for transplantation (about 1 week after the "cut" operation) as determined according to previously reported data (Barone and Feuerstein, 1999; Kelly et al., 2004), the plug was removed from the IC, leaving a well-shaped cylindrical "hole." During the transplantation operation, a suspended solution of NSCs (characterized with Nestin/Tuj/Map2/Sox1/Oct4; 10^7 cells per microliter; Figure S2) expressing GFP was slowly injected into the hole using a metallic syringe that had been inserted into the LGT. The LGT was left in place to prevent the transplanted NSCs from drifting away after transplantation (Figure 1D; Figure S3). Immediately after the injection, a multi-channel extracellular single-unit recording electrode was placed in the upper part of the "hole." The electrodes were coated with an inner tube and an outer tube (Figure 1D), which assured that the electrode was located in the center of the LGT, and thus, in the center of the transplanted stem cell mass. This design was critical for making sure that the electrodes only recorded signals from the differentiated neurons and not from the surrounding host neurons.

The two monkeys used as fibroblast controls underwent the same procedures and operation. However, 2 μl of a monkey fibroblast cell suspension (10^7 cells per microliter) was transplanted into the cylindrical "hole" instead of the NSC suspension.

Multiple-Channel Single-Unit Recording System

Recordings were carried out on seven adult rhesus monkeys (*macaca mulatta*) (two of which were fibroblast controls). The electrode was a set of 16 twisted 40-μm platinum-iridium wires (~167 μm in diameter) consisting of an inner tube and outer tube to position the electrode in the center of the LGT (Figure S3C). The resistances were around 0.5 mΩ. The electrodes were inserted bilaterally into the upper surface of the transplanted NSCs. A homemade mechanical electrode with a low weight fixed on a micro-screwdriver, and with an advance distance range of 0–1.5 mm, was mounted onto the skull at each side. Neural signals collected from the electrodes were digitized at 24 bits using an analog acquisition card (PXI-4498, National Instruments) at 40 kHz.

Fibroblast Control

The two monkeys with transplanted fibroblasts were controls for the electrophysiological study. This control was designed to exclude the possibility that the signal recorded from the electrode came from host cells. These two monkeys went through the same procedure as the other experimental animals. During the recording period, their electrodes were driven down to the maximum range (1.5 mm), and no neuronal signals had been detected. Postmortem immunohistochemistry showed there were no new neurons in the fibroblast transplanted area (Figure S5). This control experiment demonstrated that the experimental design—particularly, the electrode fabrication and implantation procedure—guaranteed that the collected neuronal signals were from transplanted cells rather than host neurons.

Sound Stimulation Recording Paradigm on Awake Monkeys

After a 2-week recovery from the stem cell transplantation, neural signals from the engrafted cells in the five experimental monkeys were recorded from 2:00 to 5:00 p.m. on a daily basis. The awake monkey was habituated to sitting quietly in a monkey chair placed in a soundproof chamber, with the background noise level below 35 dB. This background level was maintained during the whole recording period. The multiple-channel single-unit recording of the five monkeys lasted for a period of 18–22 weeks, with the electrodes being moved down slowly from time to time to search for firing neurons. The animal was randomly rewarded with drops of sugar water during recording.

Acoustic signals were generated digitally by the Adobe Audition 3.0 software (Adobe) and delivered to the soundproof chamber through a loudspeaker located 50 cm behind the animal. Two types of sound stimuli were used in the experiments: (1) pure tones of different frequencies and intensities and (2) wideband white noises of different standardized intensities, which allowed the intensity of the white noise to be consistent during its whole presenting period. Once a clear response to any sound stimuli was determined, coding characteristics of the neuron were examined using the following procedures. (1) The frequency response area was determined by changing frequency of

pure tone. Based on each neuron's feature, testing frequencies varied within a range of 200 to 10000 Hz and with steps ranging from 100 to 2500 Hz in this test (Figures 5B–5I). The first monkey was tested under an intensity of 95 dB, and the other four monkeys were tested under 80 dB. (2) Rate level function was determined by changing sound intensity levels of the white noise (Figures 5K–5S). The range of intensity changed from 60 to 95 dB by 5 dB at each step. (3) Adaptation was tested by repeating preferred sound stimulus at 80 dB (Figure 6).

All sound stimuli were presented as a tone burst with durations of 50 or 200 ms (the 50-ms stimuli were only presented to the first monkey, M07403). In the frequency response area and rate level function tests, the intervals among the tone bursts were 3–5 s and were varied randomly. In the adaptation test, 60 repetitions of the most preferred acoustic stimuli were delivered (200-ms duration, 1- to 3-s intervals). The 60 repetitions were divided into three blocks during offline analyzing. Each block contained 20 repeats, and the mean values of firing rate were calculated for each block respectively.

Offline Spike Detection and Spike Sorting

The digital signals were band-pass filtered between 0.5 and 5 kHz, and spikes were detected when the signal-to-noise ratio was over 2.0. For spike sorting, the voltage waveforms were aligned directly using a waveform peak. Spikes with similar waveforms were eyeballed and picked up as one cluster (one neuron), and the rest of waves with apparent differences from the cluster were eliminated.

For each neuron, raster plots were binned into 1 ms with a time window from 100 ms prior to the sound presentation to 300 ms after the presentation. The histograms were plotted in the same window but were binned every 5 ms. The firing rates during the 200-ms stimulus presentation time were used for the scatterplots.

Electrophysiological data collection and analysis programs were programmed with Labview (National Instruments) and displayed with Graphpad 5.1 (GraphPad Software).

Differentiated Neurons Auditory Response Activity Assessed with c-Fos Expression

After the electrophysiological experiments were finished, the monkeys were separated randomly into two groups and put in anechoic chambers. The first group, containing three monkeys, was placed individually in the chamber without sound stimuli for 2 hr prior to being exposed to a wide-band white-noise auditory stimulus (80 dB) for 30 min. Then, the monkeys were kept in the chamber without sound stimuli for another 90 min. The second group, containing two monkeys, was placed individually in the anechoic chamber without any sound stimuli for 4 hr. After the 4-hr periods, all animals were immediately sacrificed, and the brain tissues were fixed in 4% paraformaldehyde. Immunohistochemistry of c-*fos* was performed as described later. c-Fos-positive cells were counted using the CellSens Dimension software (Olympus).

Immunohistochemistry

The brains were collected and postfixed for 4 hr at 4°C, then they were cryoprotected in 30% sucrose and sectioned into 10-μm-thick slices. The slices were permeabilized with 0.2% Triton X-100 for 40 min and blocked with 5% BSA for 1 hr at room temperature. Slides were then incubated with primary antibodies at 4°C overnight. The sections were then washed three times and incubated with secondary antibodies for 2 hr at 37°C.

The transplanted cells were identified with GFP fluorescence. For different purposes, GFP-positive cells were later double stained with antibodies to Map2, NeuN, Tau, Synapsin I, PSD95, c-*fos*, and GFAP (glial fibrillary acidic protein). The sections were mounted with DAPI containing mounting solution. The slides were examined with an Olympus FV1000 fluorescence microscope. Information pertaining to the primary and secondary antibodies is presented in Tables S3 and S4, respectively.

Statistics

A t test was performed for c-*fos* immunohistochemical data with GraphPad Prism 5.1 (GraphPad Software). Significance was set at $p < 0.01$.

SUPPLEMENTAL INFORMATION

Supplemental Information includes five figures and five tables and can be found with this article online at http://dx.doi.org/10.1016/j.celrep.2016.06.066.

AUTHOR CONTRIBUTIONS

X.H., Z.W., S.Y., J.L., Y. Yao, and L. Xu initiated the project, designed the experiments, and wrote the manuscript. X.H. organized and supervised the whole project. Z.W. organized and supervised all monkey work. S.Y. organized and supervised the monkey model work. Z.W. performed the cell culture. Z.W., W.W., J. Wei, and R.Z. performed IC lesion model, single-neuron recording, and data analysis etc. Y.Z. collected data, wrote program codes, and performed data analysis. Y. Yin performed the monkey surgery. L. Li, L.X., and L. Liu performed the IC localization. Y.H., J. Wu, L.Y., H.L., D.Q., and X.F. assisted in monkey work. M.P. and A.G. edited the manuscript. J.R. provided advice and wrote and edited the manuscript. W.W., J. Wei, and R.Z. contributed equally to this work.

ACKNOWLEDGMENTS

We thank Dr. Robert Desimone from MIT and Dr. Gong Chen from PSU for their valuable suggestions on the manuscript. This research was supported by the National Program for Key Basic Research Project (973 Programs 2015CB755605, 2012CB825503, and 2012CBA01304), the Strategic Priority Research Program of CAS (XDB02020005), the Key Research Program of the Chinese Academy of Sciences, the Selected Frontier Scientific Significant Breakthrough Project of CAS, the Key Program of the Chinese Academy of Sciences (KZCC-EW-103-2), the Training Program of the Major Research Plan of the National Natural Science Foundation of China (91332120), the National Natural Science Foundation of China (81471312, 31271167, 81271495, and 81460352), the Yunnan Provincial Project to Attract One-hundred Exceptional Talents From Overseas, and the Applied Basic Research Programs of Science and Technology Commission Foundation of Yunnan Province (2014FA047).

Received: March 9, 2015
Revised: January 6, 2016
Accepted: June 15, 2016
Published: July 14, 2016

REFERENCES

Barone, F.C., and Feuerstein, G.Z. (1999). Inflammatory mediators and stroke: new opportunities for novel therapeutics. J. Cereb. Blood Flow Metab. *19*, 819–834.

Benninger, F., Beck, H., Wernig, M., Tucker, K.L., Brüstle, O., and Scheffler, B. (2003). Functional integration of embryonic stem cell-derived neurons in hippocampal slice cultures. J. Neurosci. *23*, 7075–7083.

Blurton-Jones, M., Kitazawa, M., Martinez-Coria, H., Castello, N.A., Müller, F.J., Loring, J.F., Yamasaki, T.R., Poon, W.W., Green, K.N., and LaFerla, F.M. (2009). Neural stem cells improve cognition via BDNF in a transgenic model of Alzheimer disease. Proc. Natl. Acad. Sci. USA *106*, 13594–13599.

Borisyuk, A., Semple, M.N., and Rinzel, J. (2002). Adaptation and inhibition underlie responses to time-varying interaural phase cues in a model of inferior colliculus neurons. J. Neurophysiol. *88*, 2134–2146.

Breunig, J.J., Haydar, T.F., and Rakic, P. (2011). Neural stem cells: historical perspective and future prospects. Neuron *70*, 614–625.

Englund, U., Bjorklund, A., Wictorin, K., Lindvall, O., and Kokaia, M. (2002). Grafted neural stem cells develop into functional pyramidal neurons and integrate into host cortical circuitry. Proc. Natl. Acad. Sci. USA *99*, 17089–17094.

Ferreira, A., and Rapoport, M. (2002). The synapsins: beyond the regulation of neurotransmitter release. Cell. Mol. Life Sci. *59*, 589–595.

Fuortes, M.G., Frank, K., and Becker, M.C. (1957). Steps in the production of motoneuron spikes. J. Gen. Physiol. *40*, 735–752.

Gutman, A., and Wasylyk, B. (1991). Nuclear targets for transcription regulation by oncogenes. Trends Genet. *7*, 49–54.

Hebb, D.O. (1949). The Organization of Behavior: A Neuropsychological Theory (Erlbaum).

Humphrey, D.R., and Schmidt, E.M. (1990). Extracellular single-unit recording methods. In Neurophysiological Techniques: Applications to Neural Systems, Alan A. Boulton, G.B. Baker, and Case H. Vanderwolf, eds. (Clifton, NJ: Humana Press), pp. 1–64.

Hunt, C.A., Schenker, L.J., and Kennedy, M.B. (1996). PSD-95 is associated with the postsynaptic density and not with the presynaptic membrane at forebrain synapses. J. Neurosci. *16*, 1380–1388.

Jing, W., Wenchao, W., Lin, L., Li, L., Guimei, W., Heng, T., Huihui, J., Jianhong, W., Yuanye, M., and Xintian, H. (2010). A new MRI approach for accurately implanting microelectrodes into deep brain structures of the rhesus monkey (Macaca mulatta). J. Neurosci. Methods *193*, 203–209.

Kelly, S., Bliss, T.M., Shah, A.K., Sun, G.H., Ma, M., Foo, W.C., Masel, J., Yenari, M.A., Weissman, I.L., Uchida, N., et al. (2004). Transplanted human fetal neural stem cells survive, migrate, and differentiate in ischemic rat cerebral cortex. Proc. Natl. Acad. Sci. USA *101*, 11839–11844.

Lu, P., Jones, L.L., Snyder, E.Y., and Tuszynski, M.H. (2003). Neural stem cells constitutively secrete neurotrophic factors and promote extensive host axonal growth after spinal cord injury. Exp. Neurol. *181*, 115–129.

McAlpine, D., Jiang, D., and Palmer, A.R. (2001). A neural code for low-frequency sound localization in mammals. Nat. Neurosci. *4*, 396–401.

Miyata, S., Tsujioka, H., Itoh, M., Matsunaga, W., Kuramoto, H., and Kiyohara, T. (2001). Time course of Fos and Fras expression in the hypothalamic supraoptic neurons during chronic osmotic stimulation. Brain Res. Mol. Brain Res. *90*, 39–47.

Pankratz, M.T., Li, X.J., Lavaute, T.M., Lyons, E.A., Chen, X., and Zhang, S.C. (2007). Directed neural differentiation of human embryonic stem cells via an obligated primitive anterior stage. Stem Cells *25*, 1511–1520.

Rosahl, T.W., Geppert, M., Spillane, D., Herz, J., Hammer, R.E., Malenka, R.C., and Südhof, T.C. (1993). Short-term synaptic plasticity is altered in mice lacking synapsin I. Cell *75*, 661–670.

Rossi, F., and Cattaneo, E. (2002). Opinion: neural stem cell therapy for neurological diseases: dreams and reality. Nat. Rev. Neurosci. *3*, 401–409.

Ryan, A., and Miller, J. (1978). Single unit responses in the inferior colliculus of the awake and performing rhesus monkey. Exp. Brain Res. *32*, 389–407.

Sahni, V., and Kessler, J.A. (2010). Stem cell therapies for spinal cord injury. Nat. Rev. Neurol. *6*, 363–372.

Schnupp, J.W., and King, A.J. (1997). Coding for auditory space in the nucleus of the brachium of the inferior colliculus in the ferret. J. Neurophysiol. *78*, 2717–2731.

Southwell, D.G., Nicholas, C.R., Basbaum, A.I., Stryker, M.P., Kriegstein, A.R., Rubenstein, J.L., and Alvarez-Buylla, A. (2014). Interneurons from embryonic development to cell-based therapy. Science *344*, 1240622.

Thuret, S., Moon, L.D., and Gage, F.H. (2006). Therapeutic interventions after spinal cord injury. Nat. Rev. Neurosci. *7*, 628–643.

van Praag, H., Schinder, A.F., Christie, B.R., Toni, N., Palmer, T.D., and Gage, F.H. (2002). Functional neurogenesis in the adult hippocampus. Nature *415*, 1030–1034.

Weick, J.P., Liu, Y., and Zhang, S.C. (2011). Human embryonic stem cell-derived neurons adopt and regulate the activity of an established neural network. Proc. Natl. Acad. Sci. USA *108*, 20189–20194.

Wernig, M., Benninger, F., Schmandt, T., Rade, M., Tucker, K.L., Büssow, H., Beck, H., and Brüstle, O. (2004). Functional integration of embryonic stem cell-derived neurons in vivo. J. Neurosci. *24*, 5258–5268.

Wianny, F., Bernat, A., Huissoud, C., Marcy, G., Markossian, S., Cortay, V., Giroud, P., Leviel, V., Kennedy, H., Savatier, P., and Dehay, C. (2008). Derivation and cloning of a novel rhesus embryonic stem cell line stably expressing tau-green fluorescent protein. Stem Cells *26*, 1444–1453.

Wu, J., Wang, W., Rizak, J.D., Wang, Z., Wang, J., Feng, X., Dong, J., Li, L., Liu, L., Xu, L., et al. (2014). A new method for piercing the tentorium cerebelli for implanting fragile electrodes into the brain stem in the rhesus monkey (Macaca mulatta). J. Neurophysiol. *111*, 1027–1032.

Zhou, F.W., Fortin, J.M., Chen, H.X., Martinez-Diaz, H., Chang, L.J., Reynolds, B.A., and Roper, S.N. (2015). Functional integration of human neural precursor cells in mouse cortex. PLoS ONE *10*, e0120281.

Zwiers, M.P., Versnel, H., and Van Opstal, A.J. (2004). Involvement of monkey inferior colliculus in spatial hearing. J. Neurosci. *24*, 4145–4156.

Cell Reports, Volume *16*

Supplemental Information

Neurons Differentiated from Transplanted Stem Cells Respond Functionally to Acoustic Stimuli in the Awake Monkey Brain

Jing-kuan Wei, Wen-chao Wang, Rong-wei Zhai, Yu-hua Zhang, Shang-chuan Yang, Joshua Rizak, Ling Li, Li-qi Xu, Li Liu, Ming-ke Pan, Ying-zhou Hu, Abdelaziz Ghanemi, Jing Wu, Li-chuan Yang, Hao Li, Long-bao Lv, Jia-li Li, Yong-gang Yao, Lin Xu, Xiao-li Feng, Yong Yin, Dong-dong Qin, Xin-tian Hu, and Zheng-bo Wang

Neurons Differentiated from Transplanted Stem Cells Respond Functionally to Acoustic Stimuli in the Awake Monkey Brain

Jing-kuan Wei[1, 6, 7], Wen-chao Wang[1, 6, 7], Rong-wei Zhai[1, 6, 7], Yu-hua Zhang[1], Shang-chuan Yang[1], Joshua Rizak[1], Ling Li[3], Li-qi Xu[3], Li Liu[3], Ming-ke Pan[1], Ying-zhou Hu[1], Abdelaziz Ghanemi[1], Jing Wu[1], Li-chuan Yang[1], Hao Li[1], Long-bao Lv[4], Jia-li Li[1], Yong-gang Yao[1, 2], Lin Xu[1, 2], Xiao-li Feng[1], Yong Yin[5], Dong-dong Qin[1], Xin-tian Hu[1, 2, 4, 8] , Zheng-bo Wang[1, 8]

[1] Key Laboratory of Animal Models and Human Disease Mechanisms of Chinese Academy of Sciences & Yunnan Province, Kunming Institute of Zoology, Kunming, Yunnan, 650223, China

[2] CAS Center for Excellence in Brain Science and Intelligence Technology, Chinese Academy of Sciences, Shanghai, 200031, China

[3] Kunming General Hospital of PLA Medical Imaging Department, Kunming, Yunnan, 650032, China

[4] Kunming Primate Research Center, Kunming Institute of Zoology, Chinese Academy of Sciences, Kunming, Yunnan, 650223, China

[5] Department of Rehabilitation Medicine, the Fourth Affiliated Hospital of Kunming Medical University, Kunming, Yunnan, 650021, China

[6] Kunming College of Life Science, University of Chinese Academy of Sciences, Kunming, Yunnan, 650204, China

[7] These authors contributed equally to this work.
[8] Correspondence: wangzb@mail.kiz.ac.cn (Z.W.), xthu@mail.kiz.ac.cn (X.H.)

Supplementary

Table S1. Related to Figure S3, 4. The size of the transplanted tissues in the five monkey IC.

Animals' ID	M09311	M07437	M07409	M07403	M08001	Average
Depth (mm)	2.77	2.02	2.64	2.22	3.02	2.53
Diameter (mm)	1.89	1.82	1.77	1.82	1.92	1.84
Electrode ending depth (mm)	1.0	1.0	0.906	1.0	1.5	N/A

Table S2. Related to Figure 4, 5 and 6. Electrophysiological data of all the neurons from the five monkeys.

Animal ID	M09311	M07437	M07409	M07403	M08001
Number of Total Neurons	9	1	1	3	5
Stimuli-Related Neurons	m09311-3*#^ m09311-4* m09311-5*^ m09311-8#			m07403-3#	
Spontaneous Discharge Neurons	m09311-1 m09311-2 m09311-6 m09311-7 m09311-9	m07437-1	m07409-1	m07403-1 m07403-2	m08001-1 m08001-2 m08001-3 m08001-4 m08001-5

The number after the animal ID is named in chronological order. For instance, 'm09311-3' was the third neuron recorded from M09311. '#' represents the response was frequency related. '*' represents intensity related. '^' represents an adaptive response.

Table S3. Related to Figure 2, 3 and Figure S5. Primary antibodies in alphabetical order.

Immunogen	Species/Class	Cat. No	Supplier	Dilution for ICC
c-fos	Rabbit/IgG	226 003	Synaptic system	1:200
GFAP	Mouse/IgG	SMI-21R	BioLegend	1:1000
Map2	Mouse/IgG1	M4403	Sigma	1:800
Nestin	Rabbit/IgG	AB5922	Millipore	1:200
NeuN	Mouse/IgG1	MAB377	Millipore	1:200
NeuN	Rabbit/IgG	ABN78	Millipore	1:200
Oct4	Rabbit/IgG	Ab18976	Abcam	1:200
PSD95	Mouse/IgG1	Ab2723	Abcam	1:500
Sox1	Rabbit/IgG	Ab87775	Abcam	1:800
Synapsin	Rabbit/IgG	S193	sigma	1:800
Tau	Mouse/IgG1	ab12357	Abcam	1:800
Tuj-1	Mouse/IgG1	MAB1637	Millipore	1:200

Table S4. Related to Figure 2, 3 and Figure S5. Secondary antibodies.

Name	Supplier	Dilution
Goat anti-mouse IgG-cy3	sigma	1:400
Goat anti-rabbit IgG-cy3	sigma	1:400
Goat anti-rabbit IgG CFL405	Jackson	1:200
Goat anti-mouse IgG-cy5	Jackson	1:200
Donkey anti-rabbit IgG-cy5	Jackson	1:200

Table S5. Related to Figure 2J and 3C.

Figure		N（animals）	n（slices）	Avg Cell Number	SD	SEM
Fig. 2I	DAPI	5	31	1548.6	210.98	37.89
	NeuN			186.4	71.72	12.88
Fig. 6C	c-Fos (Stim)	3	8	98.0	12.14	4.29
	c-Fos (NStim)	2	9	6.7	3.42	1.14

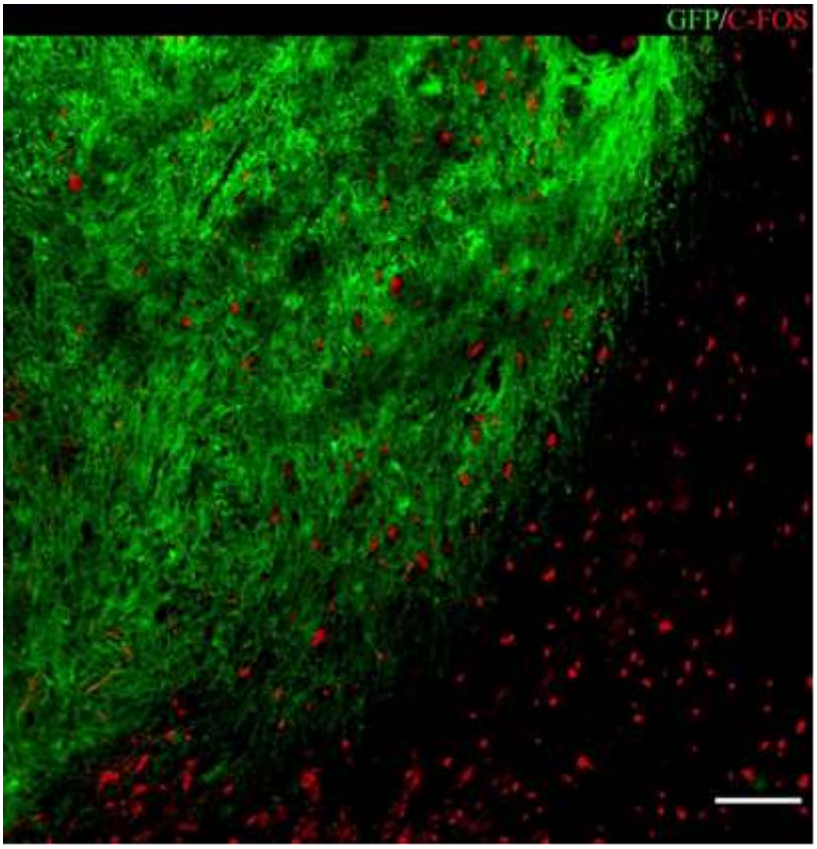

Figure S1. Related to Figure 3. The c-Fos expression in an auditory stimulated monkey. This figure shows both the transplanted area and nearby host brain area. The positive expression of c-Fos protein was about 2 fold higher in the host tissue than in the transplanted area. Scale bar: 100 μm.

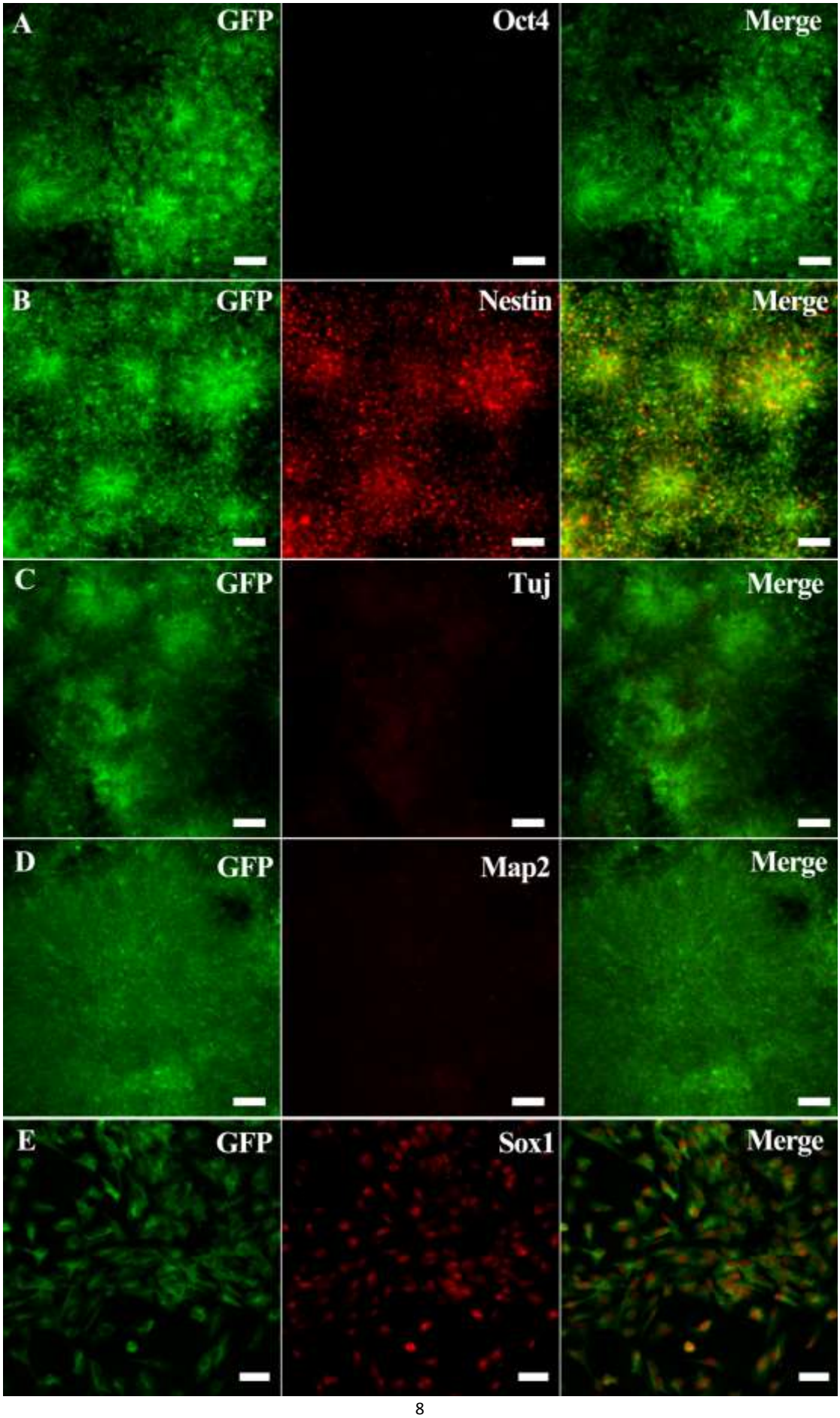
A
GFP
Oct4
Merge
B
GFP
Nestin
Merge
C
GFP
Tuj
Merge
D
GFP
Map2
Merge
E
GFP
Sox1
Merge

Figure S2. Related to Figure 1, 2. Immunocytochemistry tests for purity of NSCs.

(A) Oct4 was used to identify embryonic stem cells, and the image suggests there were almost no undifferentiated ESCs. **(B)** Nestin was used to identify NSCs, and the image suggests the majority of ESCs have differentiated into NSCs. **(C)** Beta tubulin III was used to identify neurons and the image suggests no NSCs have differentiated into neurons. **(D)** Map2 was used to identify neurons and no NSCs have differentiated into neurons. **(E)** After transplantation, Sox1 was used to identify NSCs from remaining cells and the result suggests most of cells were NSCs. Scale bars: 50 μm.

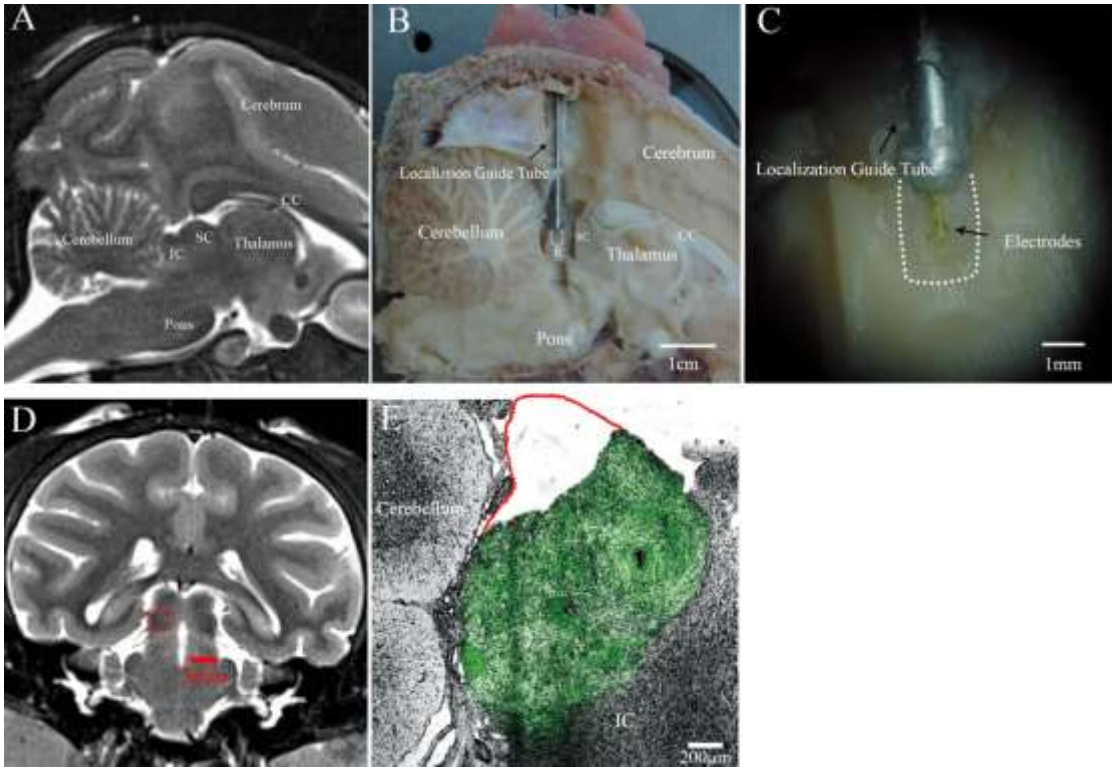

Figure S3. Related to Figure 1. MR images of the locations of IC, the electrode and a postmortem sagittal section of transplant tissue. (A) A sagittal MRI section shows the location of IC in the midbrain. **(B)** An actual photo of brain shows the location of the electrode is approximately at the same place as the IC in A. **(C)** An enlarged view of the electrode from B. The white dotted line shows the estimated area of the transplant site. **(D)** A coronal MRI section reveals IC size. The red circle indicates the left IC. The red bar is 5.00 mm in length. **(E)** A side view shows the location of the transplanted tissue, which is right next to the cerebellum and on the top of the IC. The red dotted line illustrates an estimated part of the transplanted tissue that was torn away when the electrode was taken out. SC, superior colliculus; CC, corpus callosum; IC, inferior colliculus.

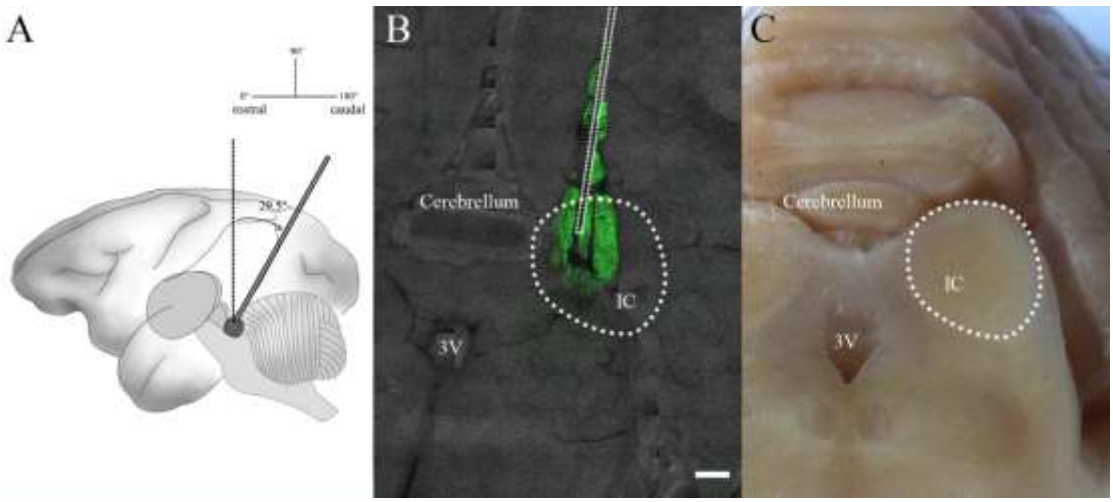

Figure S4. Related to Figure 1. Insertion angle of the Local Guide Tube and location of the transplanted tissue on the IC. (A) A schematic drawing shows the insertion angle of the localization guide tube, which was 29.5º to the posterior. **(B)** A coronal section cut at an angle tilted to the posterior by 29.5º (along the insertion track of the localization guide tube) shows the location of the transplanted tissue in the IC and the track of the electrode (white dotted line). The white dotted circle shows the estimated IC location which was identified by comparing B with C. Scale bar: 1 mm. **(C)** A coronal section of a brain stem cut at the same angle as a and b shows the location of IC relative to the third ventricle and cerebellum. This assisted with IC location in B. The telencephalon was detached from the brain stem in C, making the part differ from that of B The white dotted circle shows the IC area. 3V, third ventricle.

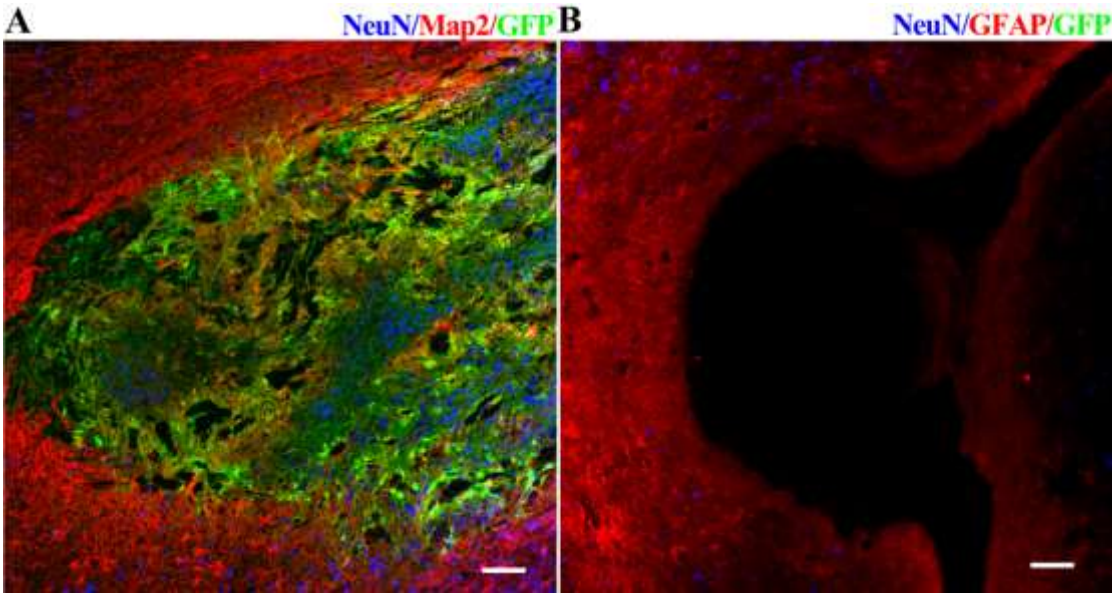

Figure S5. Related to Figure 2, 5 and 6. Comparison of the monkey IC histological sections from animals transplanted with GFP-neural stem cells and animals transplanted with monkey fibroblasts. (A) There are a substantial number of new neurons at the transplanted site in the IC in which GFP-neural stem cells had been transplanted. **(B)** No neurons or glial cells were found at the transplanted site of the IC in which monkey fibroblast cells had been transplanted. Antibodies in each image are marked above their corresponding image. Scale bar: 100 μm.

Article

Cell Reports

Neurons Differentiated from Transplanted Stem Cells Respond Functionally to Acoustic Stimuli in the Awake Monkey Brain

Graphical Abstract

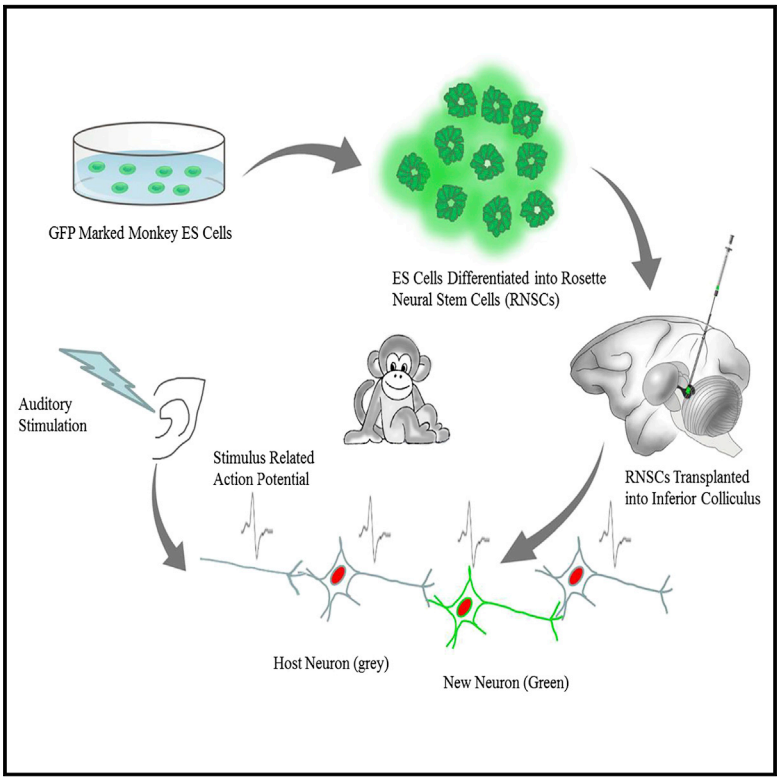

Highlights

- Stem cells were transplanted into the inferior colliculus (IC) of rhesus monkeys
- Differentiated neurons formed reciprocal anatomical connections with host neurons
- Some differentiated neurons responded to auditory stimuli in an IC-specific manner
- Transplanted stem cells likely integrated into host neural networks

Authors

Jing-kuan Wei, Wen-chao Wang, Rong-wei Zhai, ..., Dong-dong Qin, Xin-tian Hu, Zheng-bo Wang

Correspondence

xthu@mail.kiz.ac.cn (X.-t.H.), wangzb@mail.kiz.ac.cn (Z.-b.W.)

In Brief

Integration of differentiated neurons into a functioning neural network is important for the development of stem cell therapies. Wang et al. found that neurons differentiated from transplanted stem cells respond to auditory stimuli in awake monkeys after transplantation.

Wei et al., 2016, Cell Reports *16*, 1016–1025
July 26, 2016
http://dx.doi.org/10.1016/j.celrep.2016.06.066

OPEN ACCESS
CellPress

Cell Reports
Article

Neurons Differentiated from Transplanted Stem Cells Respond Functionally to Acoustic Stimuli in the Awake Monkey Brain

Jing-kuan Wei,[1,6,7] Wen-chao Wang,[1,6,7] Rong-wei Zhai,[1,6,7] Yu-hua Zhang,[1] Shang-chuan Yang,[1] Joshua Rizak,[1] Ling Li,[3] Li-qi Xu,[3] Li Liu,[3] Ming-ke Pan,[1] Ying-zhou Hu,[1] Abdelaziz Ghanemi,[1] Jing Wu,[1] Li-chuan Yang,[1] Hao Li,[1] Long-bao Lv,[4] Jia-li Li,[1] Yong-gang Yao,[1,2] Lin Xu,[1,2] Xiao-li Feng,[1] Yong Yin,[5] Dong-dong Qin,[1] Xin-tian Hu,[1,2,4,*] and Zheng-bo Wang[1,*]

[1]Key Laboratory of Animal Models and Human Disease Mechanisms of Chinese Academy of Sciences and Yunnan Province, Kunming Institute of Zoology, Kunming, Yunnan 650223, China
[2]CAS Center for Excellence in Brain Science and Intelligence Technology, Chinese Academy of Sciences, Shanghai 200031, China
[3]Medical Imaging Department, Kunming General Hospital of PLA, Kunming, Yunnan 650032, China
[4]Kunming Primate Research Center, Kunming Institute of Zoology, Chinese Academy of Sciences, Kunming, Yunnan 650223, China
[5]Department of Rehabilitation Medicine, Fourth Affiliated Hospital of Kunming Medical University, Kunming, Yunnan 650021, China
[6]Kunming College of Life Science, University of Chinese Academy of Sciences, Kunming, Yunnan, 650204, China
[7]Co-first author
*Correspondence: xthu@mail.kiz.ac.cn (X.-t.H.), wangzb@mail.kiz.ac.cn (Z.-b.W.)
http://dx.doi.org/10.1016/j.celrep.2016.06.066

SUMMARY

Here, we examine whether neurons differentiated from transplanted stem cells can integrate into the host neural network and function in awake animals, a goal of transplanted stem cell therapy in the brain. We have developed a technique in which a small "hole" is created in the inferior colliculus (IC) of rhesus monkeys, then stem cells are transplanted in situ to allow for investigation of their integration into the auditory neural network. We found that some transplanted cells differentiated into mature neurons and formed synaptic input/output connections with the host neurons. In addition, c-Fos expression increased significantly in the cells after acoustic stimulation, and multichannel recordings indicated IC specific tuning activities in response to auditory stimulation. These results suggest that the transplanted cells have the potential to functionally integrate into the host neural network.

INTRODUCTION

Neural stem cell (NSC) transplantation has been demonstrated to facilitate the recovery of functional loss resulting from neurodegenerative diseases (Rossi and Cattaneo, 2002) and/or brain/spinal cord injury (Sahni and Kessler, 2010; Thuret et al., 2006). This suggests that NSCs have therapeutic potential for such impairment, although the mechanism underlying the observed recovery is controversial. A number of researchers have attributed this recovery to the secretion of trophic factors or their derivatives by the transplanted NSCs. The trophic factors then slow or prevent the deterioration of the degenerating neurons (Blurton-Jones et al., 2009; Breunig et al., 2011; Lu et al., 2003). Alternatively, others have suggested that the neurons differentiated from the transplanted NSCs might substitute for the injured or lost neurons by functionally integrating into the host neural circuitry (Englund et al., 2002; van Praag et al., 2002; Weick et al., 2011).

Although both possibilities have potential benefits for treatment, the functional integration of transplanted NSCs into the host neural network is a cornerstone for the future of NSC clinical applications. This study was developed to examine whether transplanted NSCs can function in an awake animal brain. Here, a "cut-and-fill" technique that confines the transplanted NSCs to a small cylindrical space in rhesus monkey brain was developed (as outlined in Experimental Procedures), allowing the use of immunohistochemical and neuro-electrophysiological techniques to investigate the integration of stem-cell-derived neurons in awake animals.

The inferior colliculus (IC) was selected as the site of transplantation, since almost all IC neurons show strong responses to auditory stimuli at a wide range of intensities and frequencies (McAlpine et al., 2001; Schnupp and King, 1997). Moreover, the deep location of the IC within the brain provides a number of advantages to other brain areas, such as the primary visual cortex (V1) or the primary somatosensory cortex (S1), because it minimizes the effects of natural brain shifting and pulsations on the electrophysiological recording as well as having a higher firing rate in response to stimuli. A high firing rate in the transplant area increases the possibility of establishing new connections between the host and transplanted neurons in accordance with Hebb's law: neurons that fire together, wire together (Hebb, 1949).

RESULTS

"Cut-and-Fill" Transplantation Strategy

Post-mortem immunohistological examination of the surgery site demonstrated that the "cut-and-fill" strategy created a

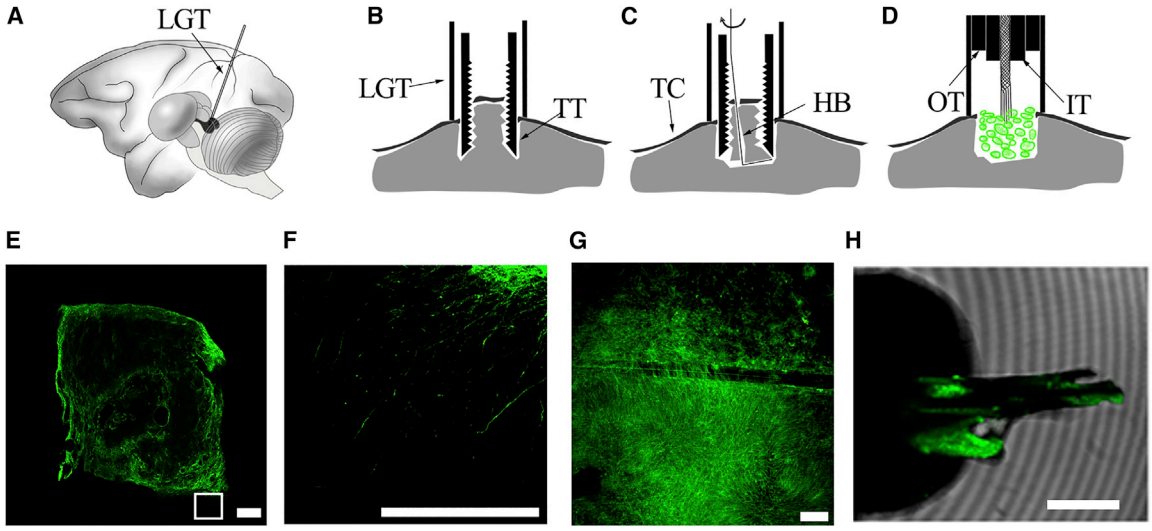

Figure 1. Schematic Diagrams Showing the Mechanical Lesion Procedure of Developing the IC Transplantation Model and GFP-Labeled Transplanted NSCs' Histological Images

(A) A localization guide tube (LGT) was inserted into the brain until it came into contact with the IC (black).

(B) A thin tube with internal threads and a sharp-toothed tip was used to make an incision on the dura membrane and to separate part of the IC tissue. TT, thin tube with internal threads and a sharp-toothed tip.

(C) A hook-shaped needle blade separated the bottom IC tissue to form a "hole." HB, hook-shaped needle blade; TC, tentorium cerebelli.

(D) A cross-section shows the transplantation of GFP-labeled NSCs and the placement of the single-unit recording electrode. IT, inner tube; OT, outer tube.

(E) A histological image showing the survival of GFP-labeled cells transplanted into a "hole" in the IC. The transplanted GFP-labeled cells have a clear boundary with the host IC tissue.

(F) A detailed view of the inset in (E) shows the projections of the transplanted NSCs into the surrounding host tissue.

(G) GFP-labeled NSCs grown in the presence of electrode for 7 days.

(H) An image of transplanted GFP-labeled cells attached to an electrode removed from a monkey IC.

Scale bars, 250 μm in (E) and (F), 50 μm in (G), and 60 μm in (H).

cylindrical "hole" with a well-defined boundary between the surrounding brain tissue in the IC and the transplanted cell mass (Figure 1E; Figure S1; Table S1). The transplanted NSCs generated a large number of fibers projecting into the surrounding brain tissue (Figure 1F; discussed later). Furthermore, the recording electrode used in this study had a good biocompatibility for at least 6 months, as indicated by the survival of many GFP-labeled cells attached to the recording electrode after its removal from the transplantation site (Figure 1H).

Transplanted NSCs Survived and Differentiated into Mature Neurons

Further immunohistochemical experiments were conducted 6 months after the transplantation to determine whether the surviving transplanted NSCs had differentiated into neurons. The cells were evaluated for classic neural markers: NeuN, Tau, and Map2 (Figures 2A–2C). Transplanted GFP+ cells were stained with NeuN/Tau or NeuN/Map2. The cells were found to have a clear formation of the nucleus and cytoskeleton, indicating differentiation into mature neurons (Figures 2A and 2B) with notable axonal projections (Figure 2C). Approximately 12.2% of the surviving transplanted NSCs had differentiated into neurons (Figures 2D and 2J), while about 29.4% of cells around the area of transplantation were found to be NeuN positive in host IC tissues (Figure 2J).

The area of transplantation was also stained with dendritic and synaptic markers to determine whether the transplanted NSCs formed neuronal connections with host neurons. Map2 staining at the edge of the transplanted site showed that there were abundant dendritic fibers sprouting into the surrounding host brain tissue (Figure 2E). Synapsin I, a major phosphoprotein found on synaptic vesicles (Ferreira and Rapoport, 2002; Rosahl et al., 1993) and a classic presynaptic membrane marker, was used to identify presynaptic terminals. Some presynaptic terminals from host neurons (Synapsin I positive, GFP negative) were identified inside the transplanted tissue (Figure 2F). These results, taken together with PSD-95 (postsynaptic density protein-95; Hunt et al., 1996)-positive staining (Figure 2I), showed that a large number of synapses originating from host neurons formed on the differentiated neurons in the site of transplantation. These synapses might provide the anatomical foundations for the host neurons to send neuronal signal outputs to the differentiated neurons.

These data also demonstrated that projections from the differentiated neurons to the host neurons were formed (Figures 2G and 2H). For example, the axons of some of the differentiated neurons (GFP-positive cells co-labeled with Tau) projected into the host tissue and sprouted around the host neurons (Figure 2G). Moreover, some presynaptic terminals from the differentiated neurons (GFP-positive cells co-labeled with Synapsin I) were identified in the host tissue (Figure 2H).

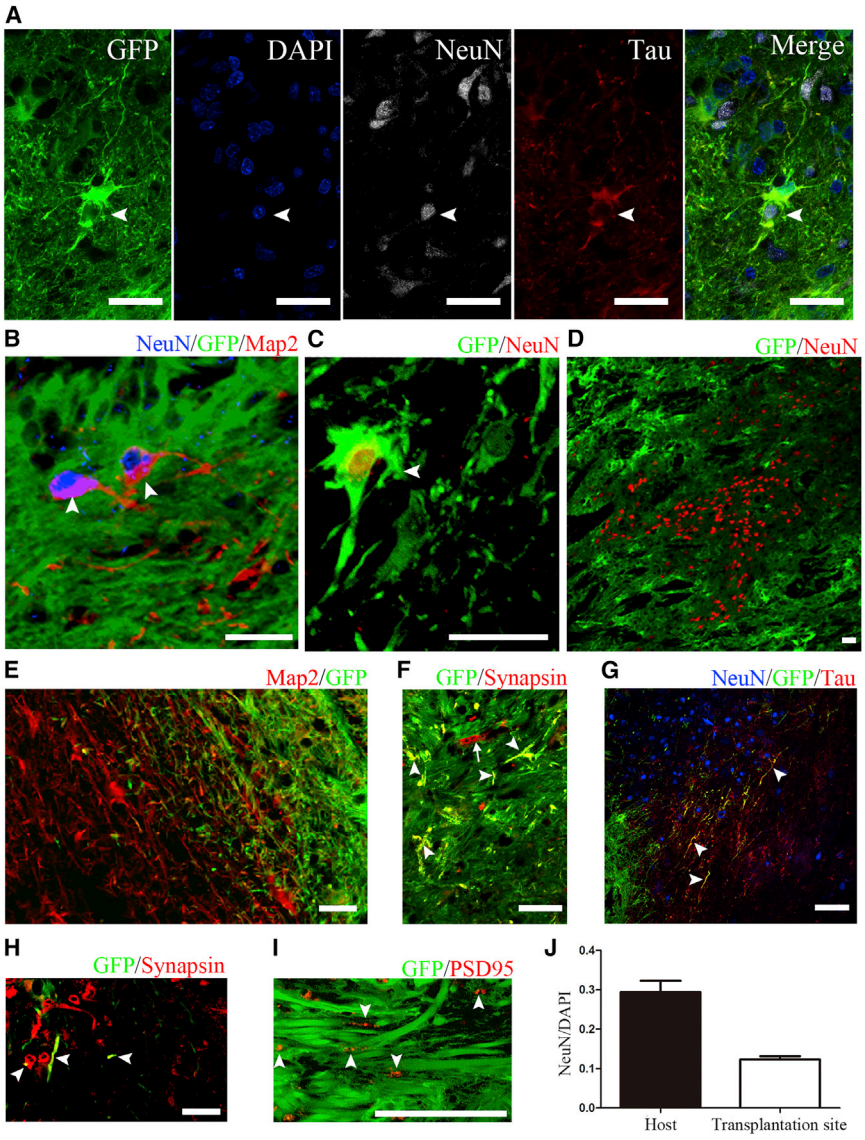

Figure 2. Transplanted NSCs Differentiated into Mature Neurons and Formed Synapses with Neighbor and Host Neurons

(A) A transplanted NSC (GFP) differentiated into a mature neuron (arrowhead; neuronal nucleus, NeuN, white; axons and other neurites, Tau, red).

(B) Two mature neurons differentiated from transplanted NSCs (arrowheads) (NeuN, blue; dentritics, Map2, red).

(C) A differentiated neuron (arrowhead) with a clear axon (NeuN, red; GFP, green).

(D) At lower magnification, a large number of transplanted NSCs differentiated into neurons (NeuN, red).

(E) The border of the transplant site. Dendritic fibers of engrafted NSCs sprouted into the host brain (Map2, red).

(F) Host (arrow) and the differentiated neuron (arrowheads) presynaptic terminals in the transplanted tissue (Synapsin I, red).

(G) Axons (arrowheads; Tau, red) of the differentiated neurons (GFP) projected around host neurons (NeuN, blue).

(H) Differentiated neurons formed presynaptic terminals (arrowheads; synapsin I, red) in the host IC.

(I) Postsynaptic terminals (arrowheads) of the differentiated neurons (PSD-95, red).

(J) The ratios of neurons (NeuN labeled) to all cells (DAPI labeled) in area of transplantation and the host IC tissues around the area in an area of 0.4 mm^2. About 12.2% of transplanted cells differentiated into neurons (n = 31), and approximately 29.4% of cells were neurons in host IC tissues around the area of transplantation (n = 17). Error bars indicate SEM. Scale bars, 30 μm. See also Table S5.

All told, these immunohistochemical data demonstrated that the NSCs survived after the transplantation, that the cells differentiated into mature neurons, and that synaptic structures were formed between the differentiated neurons and host neurons. This suggests that an anatomical and cellular basis for neuronal signals to flow into and out of the transplanted area was established.

Sound-Evoked c-Fos Expression Marks Activity of the Neurons Differentiated from the Transplanted NSCs

c-Fos, an immediate early gene and proto-oncogene, is highly expressed in active cells (Gutman and Wasylyk, 1991) and has been used as an effective tool to investigate cellular activity in the brain because the number of c-*fos*-positive neurons in an activated brain region continuously and significantly increases for 2 hr following a stimulus (Miyata et al., 2001). The monkeys in this study were given auditory stimulation to induce auditory responses from the differentiated neurons in the IC, and c-*fos* expression was used to demonstrate the activities. Five awake monkeys were divided into two groups and put individually into an anechoic chamber. The first group consisted of three monkeys that had been kept in the chamber without sound stimulation for 2 hr followed by exposure to a wide band white-noise stimulus (80 dB) for 30 min. After which, the monkeys were kept in the chamber without stimulation for another 90 min. The other two monkeys (control group) were put in the same chamber without any sound stimulus for 4 hr. After the respective 4-hour periods, each animal was immediately sacrificed, and the brain tissues were fixed in 4% paraformaldehyde.

The expression of c-Fos protein in the differentiated neurons after the stimulus was identified with the co-expression of NeuN (Figures 3A and 3B). Although c-*fos* was expressed in the differentiated neurons of all five monkeys, the control group (without sound stimulus) had a significantly lower expression level in the area of transplantation than the monkeys of the sound stimulus group ($p < 0.01$) (Figure 3C). Most of the differentiated neurons in the stimulated group were c-*fos* positive (about

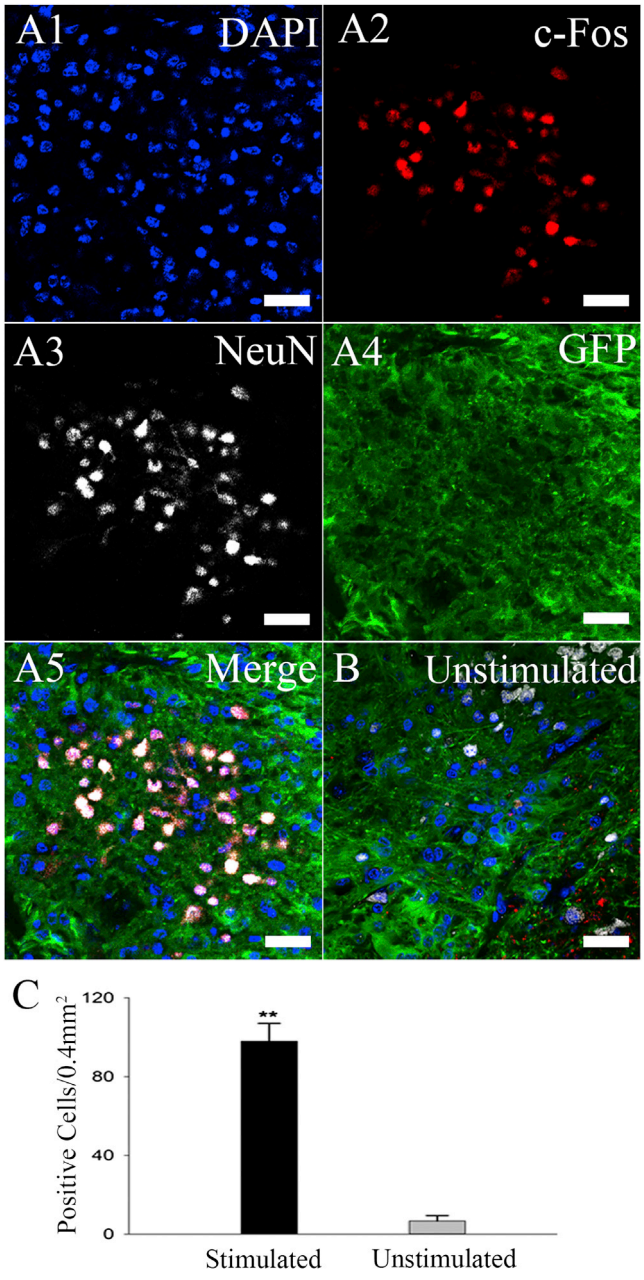

Figure 3. Comparison of c-*fos* Expression in the Differentiated Neurons in Acoustically Stimulated Monkeys and Non-stimulated Monkeys

(A) Co-labeling (NeuN/c-*fos*) of the differentiated neurons in the auditorily stimulated group (n = 3) showed high activity (arrows). A1 displays all cell nuclei stained by DAPI (blue). A2 displays active cells responding to stimulus stained by c-*fos* (red). A3 displays neuronal nuclei staining (NeuN, white). A4 displays surviving transplanted cells (GFP, green). A5 displays the merged image.

(B) Active differentiated neurons (arrow) in the non-auditorily stimulated group (n = 2) were visualized by co-labeling with NeuN (white) and c-*fos* (red).

(C) c-Fos expression in the auditorily stimulated group was significantly higher than in the non-stimulated group. **$p < 0.01$.

Error bars represent SEM. Scale bars, 30 μm. See also Table S5.

70% of the differentiated neurons were activated, i.e., GFP-positive cells co-labeled with NeuN and c-*fos*; Figures 3A1–3A5). These findings demonstrated that there were robust auditory neuronal activities among the differentiated neurons (Figure S1). This suggested that the differentiated neurons had received stimulus-evoked neuronal inputs from host IC neurons through the synaptic connections demonstrated in the immunohistochemical experiments discussed earlier. These findings suggest that, after processing these inputs, the differentiated neurons generated action potentials and then likely sent them out to host neurons in the IC through projections between them (for additional evidence, please refer to the single-neuron recording study section) and that the differentiated neurons may function in the awake animal brain.

Electrophysiological Recording from the Transplanted Area after Acute Auditory Stimulation

While the c-*fos* expression demonstrated that a substantial number of the differentiated neurons showed auditory stimulation related activities, a multi-single-neuron recording technique was used in situ to get a better observation of the firing characteristics of the differentiated neurons. The recordings were conducted in the site of transplantation of five awake monkeys after the animals were given 2 weeks to recover from the NSC transplantation surgery. Single-neuron activities were recorded under auditory stimulation for a time period of 18 to 22 weeks.

During the first 3 to 4 weeks of the recording period, no neuronal discharges were detected. From the fourth week onward, spontaneous spike signals were recorded in the upper part of the transplanted tissue in five monkeys. The electrode was not driven down further into the transplanted mass until spontaneous activity had been observed in the IC. This time course is consistent with previously reported time frames for engrafted stem cells to differentiate into functional neurons (Southwell et al., 2014). This suggests that the first 6 weeks after transplantation might be an important time period for the transplanted NSCs to differentiate into mature neurons.

After the fourth week, up to the 22nd week, the electrode was gradually moved down to record from the differentiated neurons. By the end of the recording period, a total of 19 neurons were recorded in the five awake monkeys (Table S2). Five of these 19 neurons showed clear responses to the auditory stimuli. Typical responses of three neurons are shown in Figure 4B. The waveforms of the spikes were similar to the characteristics of a typical cell-body spike's waveform rather than those of an axon's waveform (Figures 4C, 5A, and 5J) (Fuortes et al., 1957; Humphrey and Schmidt, 1990). Each waveform had an obvious hyperpolarization and lasted for a duration of 1 ms. This characteristic was observed from all 19 neurons. The spikes of a representative neuron (m07403-3; Figures 4C and 4D) in response to pure tones of 8000 Hz and 95 dB was tightly correlated to the onset and offset of the auditory stimulation and had a latency around 15 ms, This latency is similar to the normal latency of IC neurons reported by Ryan and Miller (1978). This suggests that neuron m07403-3 received functional excitatory inputs from host neurons and integrated them before generating action potentials.

Previous studies have shown that one of the responsive characteristics of the IC neuron is that it responds optimally to a

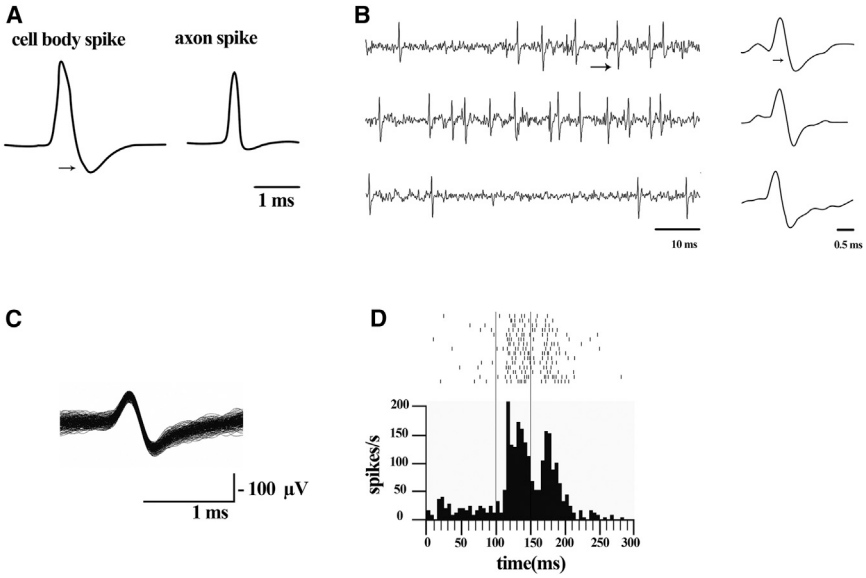

Figure 4. The Differentiated Neurons Have Typical Action Potential Waveforms of a Cell-Body Spike and Similar Auditory-Stimulus-Related Responses to Host IC Neurons

(A) Typical cell-body and axon spike voltage waveforms. The cell-body spike has an obvious hyperpolarization (arrow) and a duration of 1 ms, whereas the axon spike lacks the hyperpolarization component in the waveform and has a shorter duration (about 0.5 to 0.7 ms).

(B) Spike trains from three different somas of the differentiated neurons. They all had a clear hyperpolarization phase (arrows) and lasted for a duration of 1 ms.

(C) The voltage waveforms recorded from a differentiated neuron (m07403-3) when the monkey was stimulated with an auditory stimulus of 8000 Hz and 95 dB.

(D) A raster plot and histogram show an atypical time-locked differentiated neuron's response (15 ms in latency) to an auditory stimulus (the vertical lines on the histogram at 100 ms and 150 ms indicate the onset and the offset of the stimulus, respectively). The spikes appeared tightly correlated to the onsets and offsets of the auditory stimulation with a latency around 15 ms, which is similar to the normal latency of a host IC neuron.

specific frequency (an optimum frequency) (Zwiers et al., 2004). To determine the individual optimum frequency of five differentiated neurons that displayed clear responses to the auditory stimuli, the auditory responses of the five neurons were further tested, with pure tones at different frequencies ranging from 200 Hz to 10000 Hz at an intensity of 80 dB. The recordings from neuron m09311-3 (located less than 1 mm under the IC surface; Figure 5B) showed that it had a typical responsive frequency area and its optimal frequency was 2,000 Hz (Figures 5C–5I). This activity is similar to previously reported data recorded from neurons located 1 mm under the IC subsurface (Zwiers et al., 2004). This suggests that neuron m09311-3 did not randomly respond to the stimuli and had acquired certain local properties of the IC, especially in terms of stimulus frequency selectivity.

In addition to frequency tests, the differentiated neurons were also examined for how they responded to changes in sound intensity. In the experiments, the monkeys were exposed to white noise with different intensities (60, 65, 70, 75, 80, 85, 90, and 95 dB). Three neurons were found to be monotonic to the sound intensity changes, and the responses from a representative neuron (m09311-4) are shown in Figures 5K–5S. This indicated that their firing rates increased with the increment of sound intensity. This property has been reported as a typical feature of IC neurons (Zwiers et al., 2004).

Among the 19 neurons recorded from the five monkeys, five neurons showed frequency/intensity-related activities (Figure 5; Table S2). Among these five neurons, two changed their firing rates as the frequency varied, two responded monotonically to sound intensity increases, and one showed response changes to both. These results indicated that these differentiated neurons had a coding feature tuning to the external stimuli and demonstrated similar firing characteristics to previously reported IC neurons.

Another common responsive property of the IC neuron is that its responses will decline with the repetition of same auditory stimuli. This feature is a result of an adaptation of either the neuron itself or the whole neural network (Borisyuk et al., 2002). This adaptive property was observed in two differentiated neurons, which had received 60 identical auditory stimuli (The average intertrial interval [ITI] was 2 s, and each stimulus lasted for 200 ms; Figure 6). The data from a representative neuron (m09311-5) are shown in Figure 6. Its firing rate was above 20 spikes per second for the first block of 20 identical stimulations. The discharge rate decreased to approximately 17 spikes per second for the second block of 20 stimulations. For the last block of 20 stimulations, the firing rate dropped to around six spikes per second (Figure 6). These data indicated that these two differentiated neurons displayed an adaptive response property similar to that of previously reported IC neurons (Borisyuk et al., 2002).

All told, the single-neuron recording data from the site of transplantation provided details regarding the activity characteristics of the differentiated neurons. Specifically, some of the differentiated neurons exhibited tuning activities, such as tuning to frequency/intensity changes, and adapted to the repetition of auditory stimuli. These properties are similar to reported properties of IC neurons and suggest that the differentiated neurons may function in awake animals.

DISCUSSION

In this study, stem cells were transplanted into a small "hole" introduced into the IC of rhesus monkeys in order to evaluate the integration of the differentiated neurons into the host neural network. Immunohistochemical data demonstrated that the transplanted NSCs differentiated into mature neurons and formed input/output synaptic connections with host neurons.

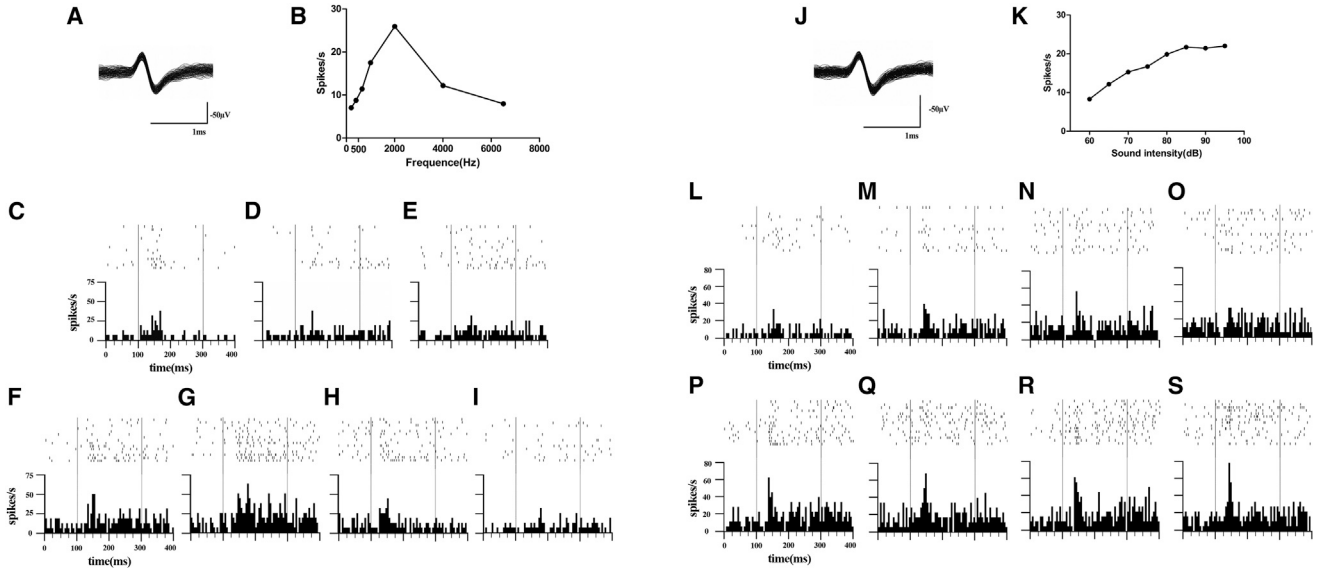

Figure 5. Responses of Differentiated Neurons to the Frequency and Intensity of Auditory Stimuli in Awake Monkeys

(A) Voltage waveforms recorded from a representative neuron (m09311-3) when the animal was stimulated with an optimized sound stimulus (2000 Hz). The waveforms have the hyperpolarization and long duration of a soma spike.

(B) Frequency response area of neuron m09311-3.The firing rates in the chart are calculated from the data in (C)–(I).

(C–I) Raster plots and histograms reveal the responses from neuron m09311-3 to pure-tone stimuli with different frequencies at an intensity of 80 dB: the responses were to frequencies at 200, 400, 650, 1000, 2000, 4000 and 6500 Hz, respectively.

(J) Voltage waveforms of a representative neuron (m9311-4) when the animal was stimulated with white noise at an intensity of 75 dB.

(K) The firing rate level function of neuron m09311-4 (white noise). The firing rates are calculated from the data in (L)–(S).

(L–S) Raster plots and histograms reveal the responses of neuron m09311-4 to white-noise stimuli with different sound levels: 60, 65, 70, 75, 80, 85, 90, and 95 dB.

This indicated that the transplanted NSCs had integrated into the host neural network. c-Fos expression was used to study the regional response of the differentiated neurons to auditory stimulation. Around 70% of the differentiated neurons showed increased c-*fos* expression after receiving auditory stimulation. This indicated that the differentiated neurons received stimulus-evoked neuronal inputs from host IC neurons. After integrating the inputs on their cell bodies, those differentiated neurons generated action potentials that, in turn, likely sent out spikes to the host neurons. In addition, a multi-channel single-neuron recording technique was used to record and illustrate neuronal activity in the site of transplantation. The recordings showed that some of the differentiated neurons displayed tuning activities similar to previously reported activities of IC neurons (Borisyuk et al., 2002; Zwiers et al., 2004). This indicated that the differentiated neurons received excitatory inputs and processed them in order to exhibit IC-specific tuning activities and responses. All of these findings suggest that the transplanted NSCs have the potential to integrate into the host neural network and function in the awake animal brain.

Previous research on the integration of neurons differentiated from stem cells into host networks has been carried out predominantly on brain slices. This research has found that engrafted embryonic stem cell (ESC)-derived neurons formed synaptical connections with host neurons and received artificially induced excitatory and inhibitory synaptic inputs from host neurons, such as electrical, glutamatergic, or GABA stimulation of the host tissue (Benninger et al., 2003; Englund et al., 2002; Wernig et al., 2004; Zhou et al., 2015). In another study performed on acute mouse brain slices, transplanted neurons differentiated from human ESCs expressing channelrhodopsin-2 were found to elicit both inhibitory and excitatory postsynaptic currents after optical stimulation and to produce postsynaptic signals in host pyramidal neurons (Weick et al., 2011). Moreover, previous reports have demonstrated that new neurons generated during adult neurogenesis in the mouse hippocampus display passive membrane properties and action potentials under current clamp on live slices (van Praag et al., 2002). These results suggested that new neurons—and, in particular, neurons differentiated from stem cells—are capable of integrating into the brain circuitry through the formation of new synapses. However, these results did not confirm functional neuronal activity and integration of the transplanted NSCs in awake animal brains.

To examinate whether transplanted NSCs can integrate into the host neural network and function in awake animals, we developed a "cut-and-fill" transplantation strategy to directly study the behavior and function of the transplanted NSCs in rhesus monkey brains. This strategy had a number of advantages over previous studies performed in brain slice investigations. This strategy utilized a brain region localization technique to target the IC with pinpoint accuracy, a mechanism to create a well-controlled and accurate lesion of the IC tissue and an effective measure to prevent the drifting or migration of the transplanted NSCs. In addition to these measures, the strategy accurately placed a multi-channel recording electrode within the transplant mass in order to directly investigate the functional integration of

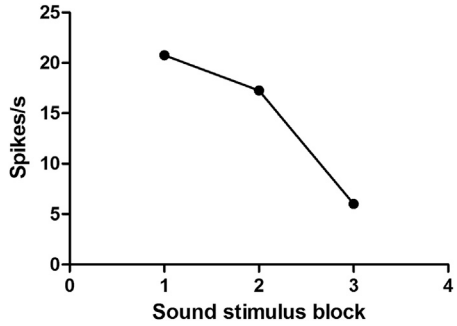

Figure 6. Adaptive Property of a Differentiated Neuron
A line chart demonstrates a decrease of firing rates of a representative neuron (m09311-5) when the monkey was stimulated by a repeated identical-sound stimulus.

the transplanted NSCs in response to specific stimuli in awake animal brains. Using this strategy, the cells were found to form anatomical connections with host neurons, to be activated by auditory stimuli, and to respond to stimuli in an IC-specific manner. This suggests that transplanted stem cells have the potential to integrate into the host neural network and function in awake animals.

Single-neuron recording was used to provide some examples and illustrate the details of firing pattern of the differentiated neurons within the transplant area. We recorded auditory responses from 19 of the neurons and found that five of them responded to the auditory stimuli in a manner similar to that of previously reported IC neurons (Borisyuk et al., 2002; Zwiers et al., 2004). The relatively low number of recorded neurons identified was partially a result of the recording being conducted within transplanted tissue, whose physiological environment and neuronal population were much different from normal brain tissue. It also should be noted that the 19 neurons had been recorded for a time period of 18 to 22 weeks. This time frame is thought to be a period when the transplanted NSCs gradually mature and integrate functionally into the host neural network. In addition, the recording electrodes had limited movement during the single-neuron recording period (as mentioned in Results), which may have also contributed to the low neuron number recorded in the area of transplantation. Nonetheless, the auditory-responsive data recorded from the five neurons that displayed IC-specific tuning properties illustrates the physiological development of synaptic connectivity and some details of the firing patterns of the neurons within the area of transplantation. Future experimentation is required to evaluate the overall auditory processing properties of the whole area of transplantation in order to gauge the full potential of the transplanted NSCs to integrate into the host neural network and function in awake animals.

While it is preliminary to fully assess the ability of transplanted stem cells to differentiate and replace lost neurons in a damaged brain, the present findings provide impetus for further, yet more sophisticated, experimentation to be conducted in order to address these important and difficult issues. This study used a "cut-and-fill" technique to investigate the functional responses of the transplanted NSCs in awake animal brains and provides a strong foundation to evaluate the full functional integration of transplanted stem cells in the future. More importantly, this study provides encouragement that further optimization of neuronal differentiation from stem cells may make stem cell replacement therapy in the brain and nervous system a reality in the not-too-distant future.

EXPERIMENTAL PROCEDURES

LYON-ESC Culture

GFP-marked rhesus monkey ESCs (a gift from the Lyon Stem Cell Research Institute; Wianny et al., 2008) were cultured in ES medium containing Knockout (KO)-DMEM (Invitrogen), 20% KO-SR (KO serum replacement) (Invitrogen), 1% nonessential amino acids (Invitrogen), 2 mM L-glutamine (Sigma-Aldrich), 0.1 mM β-mercaptoethanol (Sigma-Aldrich), and 10 ng/ml basic fibroblast growth factor (bFGF) (Invitrogen). The medium was changed every day, and mechanical passaging of undifferentiated colonies was performed manually every 5–7 days by cutting the colonies into large clumps using a flame-pulled Pasteur pipette. The LYON-ES Cs were co-cultured with mitotically inactivated mouse embryonic fibroblasts (CF-1-MEFs; ATCC). The CF-1-MEFs were first grown in DMEM (Invitrogen) with 2 mM L-glutamine supplemented with 15% FBS (Invitrogen). All cells were grown at 37°C in 5% CO_2.

NSC Induction

In order to induce NSCs, LYON-ESC colonies were digested with 1 mg/ml dispase, washed with ES medium to remove the dispase, and suspended in modified N/M medium (Pankratz et al., 2007), which contained 50% DMEM/F12 (Invitrogen), 50% neural basal medium (Invitrogen), 1 × N2 supplement (Invitrogen), 1 × B27 (Invitrogen), and 2 mM L-glutamine. Then, the cells were plated in a 15 mm × 30 mm well coated with agar (Sigma-Aldrich). The cells were allowed to aggregate for 4 days to form embryonic bodies (EBs). After this aggregation, EBs were selected and cultured in NP media in four-well plates coated with extracellular matrix (ECM; Sigma-Aldrich) for 10 to 14 days till rosette formation appeared. The NP media contained DMEM/F12, 1 × ITS-x (Invitrogen), 2 ng/ml heparin (Sigma-Aldrich), and 2 mM L-glutamine.

Neural rosette cell aggregations were then dissociated into small cell clumps by gentle pipetting. The cell suspensions were sampled and treated with trypsin (0.05% in 0.1% EDTA) for cell counting. Then, the neural rosette cells were suspended in PBS at a concentration of 10^7 cells per microliter and placed on ice for transplantation.

Monkey Fibroblast Cell Culture

Rhesus monkey fibroblasts were cultured in DMEM, containing 15% FBS and 0.1% streptomycin and gentamycin (Sigma-Aldrich) at 37°C in 5% CO_2. The cell cultures were collected and treated with trypsin (0.05% in 0.1% EDTA) for cell counting. Cells were suspended in PBS at a concentration of 10^7 cells per microliter and placed on ice for transplantation.

Immunocytochemistry of NSCs

After selection of rosette-forming cells and prior to transplantation into each monkey, a small portion of the selected cells was stained with Nestin/Tuj/Map2/Sox1/Oct4 to examine the purity of the neural progenitor population (Figure S2). The results showed that the purity of NSCs was very high and that no undifferentiated ESCs or differentiated neurons were evident. Since the ESCs and neurons were very scarce in the tests, no other NSC purifying procedure was used, except hand picking of the rosette cells. As a second confirmation, some of the grafted cells were kept to be stained after transplantation with Nestin/Tuj/Map2/Sox1/Oct4. The results were similar to the previous purity tests.

Cells for the NSC immunocytochemistry test were cultured on chamber slides and fixed in 4% paraformaldehyde (Sigma-Aldrich) in PBS for 20 min and then permeabilized with 0.1% Triton X-100 (Sigma-Aldrich) for 15 min. The slides were then blocked for 1 hr at room temperature in PBS containing 5% BSA (Sigma-Aldrich). Samples were then incubated in blocking buffer (1% BSA) containing primary antibody overnight at 4°C. Following three 5-min washings with PBS, cells were then incubated with secondary antibodies conjugated with Texas Red (1:200, Sigma-Aldrich) for 2 hr at 37°C. The samples

were washed using the same procedure as mentioned earlier and mounted with DAPI (Dako) containing mounting solution.

The following primary antibodies were used: Tubulin Beta III, Nestin, Map2, Sox1, and Oct4. Fluorescent samples were examined with a FV1000 fluorescence microscope (Olympus). The information of primary and secondary antibodies is presented, respectively, in Tables S3 and S4.

Biocompatibility Test of Polyimide-Film-Coated Electrodes with Cultured Monkey NSCs

Five platinum-iridium wires (2 mm in length, 25 μm in diameter) were placed in a dish where the rosette-shaped NSCs were cultured. Results showed that the wires exerted no significant cytotoxicity on the cells. The cells had adhered to the surface of the wire electrodes, and no obvious deformation of the attached cells was observed (Figure 1G). This suggested that the growth and proliferation of the cultured cells was not affected by the polyimide-film-coated wire electrodes.

"Cut-and-Fill" Transplantation Strategy: IC Lesion Surgery, NSC Transplantation, and Electrode Implantation

Seven (two of fibroblast control) rhesus monkeys (*Macaca mulatta*, 4–6 years old, weighing 6.5–7.5 kg) were used in this study. The monkeys were purchased from the breeding colonies of Kunming Primate Research Center, Kunming Institute of Zoology, Chinese Academy of Sciences.

All animal procedures conformed to the requirements of the Animal Welfare Act (People's Republic of China) and were approved by the Institutional Animal Care and Use Committee (IACUC) of the Kunming Institute Zoology, Chinese Academy of Sciences (Approval ID: SMKX-2016014).

An MRI-guided location technique with an accuracy of 0.5 mm developed previously in our lab (Jing et al., 2010) was used for each monkey to accurately locate the IC, a small nucleus deep in the monkey midbrain. After being anesthetized with hydrochloric acidulated ketamine (10 mg/kg, intramuscularly [i.m.]) and maintained with sodium pentobarbital (20 mg/kg, i.m.), each monkey's head was mounted on a stereotaxic apparatus (Shenzhen Reward Life Science). Three MRI-visible external markers (three rigid glass tubes, with 0.5 mm internal diameters, filled with a vitamin AD solution that is visible in the MRI) were anchored on each monkey's skull with dental acrylic. The surgery to attach the external MRI markers and specific MRI parameters has been outlined in detail previously (Jing et al., 2010). Of note, the orientation of the MRI images was set to correspond to the monkey's head within the stereotaxic frame by adjusting the scanning angle to scan through the plane of two of the three markers, which were placed on the calvarial sagittal suture, during the MRI capture. The third marker was placed near the IC location, as estimated according to an anatomical atlas of rhesus monkey brain. The relative coordinates of the IC in relation to the three external markers were later determined from MRI images of each monkey (Figure S3A).

Based on the relative IC coordinates obtained from the MRI, a localization guide tube (LGT) with an inner diameter of 1.5 mm was inserted into the monkey's brain obliquely, making it perpendicular to the IC surface. Then, a thin probe was inserted into the brain through the LGT to measure the depth of the targeted IC surface from the skull. This approach was based on a technique developed previously in our lab to pierce the tentorium cerebelli (TC) covering the IC (Wu et al., 2014). When the probe reached the surface of the IC, it recoiled due to the surface tension of the dura matter, thereby confirming the depth of the IC surface from the skull of each individual monkey. Then, the LGT was driven down to this measured depth and anchored onto the skull with dental cement. This precise placement of the LGT helped to accurately locate the lesion site on the IC (Figures S3B, S3C, S3E, and S4B). Then a mechanical separator was used to make a lesion into the IC. The separator consisted of a hook-shaped needle blade and a thin tube with an internal thread and a sharp-toothed tip. The thin tube was 2 mm longer than the LGT. First, the thin tube was gently put into the LGT until it reached the TC. By rotating the thin tube, its sharp-toothed tip cut off the TC and went down to its final depth (2 mm longer than the LGT) (Figure 1B). Then, a hook-shaped needle blade was inserted into the thin tube, and the IC tissue within the tube was cut off and removed by rotating the needle blade (Figure 1C). After this mechanical "cut" operation, a cylindrical "hole" (1.5 mm in diameter; about 2 mm in depth) in the IC was created. To prevent changes in both the size and shape of the "hole," a stainless steel plug (2 mm longer than the LGT) was inserted to fill the "hole."

When the environment in the hole was optimum for transplantation (about 1 week after the "cut" operation) as determined according to previously reported data (Barone and Feuerstein, 1999; Kelly et al., 2004), the plug was removed from the IC, leaving a well-shaped cylindrical "hole." During the transplantation operation, a suspended solution of NSCs (characterized with Nestin/Tuj/Map2/Sox1/Oct4; 10^7 cells per microliter; Figure S2) expressing GFP was slowly injected into the hole using a metallic syringe that had been inserted into the LGT. The LGT was left in place to prevent the transplanted NSCs from drifting away after transplantation (Figure 1D; Figure S3). Immediately after the injection, a multi-channel extracellular single-unit recording electrode was placed in the upper part of the "hole." The electrodes were coated with an inner tube and an outer tube (Figure 1D), which assured that the electrode was located in the center of the LGT, and thus, in the center of the transplanted stem cell mass. This design was critical for making sure that the electrodes only recorded signals from the differentiated neurons and not from the surrounding host neurons.

The two monkeys used as fibroblast controls underwent the same procedures and operation. However, 2 μl of a monkey fibroblast cell suspension (10^7 cells per microliter) was transplanted into the cylindrical "hole" instead of the NSC suspension.

Multiple-Channel Single-Unit Recording System

Recordings were carried out on seven adult rhesus monkeys (*macaca mulatta*) (two of which were fibroblast controls). The electrode was a set of 16 twisted 40-μm platinum-iridium wires (~167 μm in diameter) consisting of an inner tube and outer tube to position the electrode in the center of the LGT (Figure S3C). The resistances were around 0.5 mΩ. The electrodes were inserted bilaterally into the upper surface of the transplanted NSCs. A homemade mechanical electrode with a low weight fixed on a micro-screwdriver, and with an advance distance range of 0–1.5 mm, was mounted onto the skull at each side. Neural signals collected from the electrodes were digitized at 24 bits using an analog acquisition card (PXI-4498, National Instruments) at 40 kHz.

Fibroblast Control

The two monkeys with transplanted fibroblasts were controls for the electrophysiological study. This control was designed to exclude the possibility that the signal recorded from the electrode came from host cells. These two monkeys went through the same procedure as the other experimental animals. During the recording period, their electrodes were driven down to the maximum range (1.5 mm), and no neuronal signals had been detected. Postmortem immunohistochemistry showed there were no new neurons in the fibroblast transplanted area (Figure S5). This control experiment demonstrated that the experimental design—particularly, the electrode fabrication and implantation procedure—guaranteed that the collected neuronal signals were from transplanted cells rather than host neurons.

Sound Stimulation Recording Paradigm on Awake Monkeys

After a 2-week recovery from the stem cell transplantation, neural signals from the engrafted cells in the five experimental monkeys were recorded from 2:00 to 5:00 p.m. on a daily basis. The awake monkey was habituated to sitting quietly in a monkey chair placed in a soundproof chamber, with the background noise level below 35 dB. This background level was maintained during the whole recording period. The multiple-channel single-unit recording of the five monkeys lasted for a period of 18–22 weeks, with the electrodes being moved down slowly from time to time to search for firing neurons. The animal was randomly rewarded with drops of sugar water during recording.

Acoustic signals were generated digitally by the Adobe Audition 3.0 software (Adobe) and delivered to the soundproof chamber through a loudspeaker located 50 cm behind the animal. Two types of sound stimuli were used in the experiments: (1) pure tones of different frequencies and intensities and (2) wideband white noises of different standardized intensities, which allowed the intensity of the white noise to be consistent during its whole presenting period. Once a clear response to any sound stimuli was determined, coding characteristics of the neuron were examined using the following procedures. (1) The frequency response area was determined by changing frequency of

pure tone. Based on each neuron's feature, testing frequencies varied within a range of 200 to 10000 Hz and with steps ranging from 100 to 2500 Hz in this test (Figures 5B–5I). The first monkey was tested under an intensity of 95 dB, and the other four monkeys were tested under 80 dB. (2) Rate level function was determined by changing sound intensity levels of the white noise (Figures 5K–5S). The range of intensity changed from 60 to 95 dB by 5 dB at each step. (3) Adaptation was tested by repeating preferred sound stimulus at 80 dB (Figure 6).

All sound stimuli were presented as a tone burst with durations of 50 or 200 ms (the 50-ms stimuli were only presented to the first monkey, M07403). In the frequency response area and rate level function tests, the intervals among the tone bursts were 3–5 s and were varied randomly. In the adaptation test, 60 repetitions of the most preferred acoustic stimuli were delivered (200-ms duration, 1- to 3-s intervals). The 60 repetitions were divided into three blocks during offline analyzing. Each block contained 20 repeats, and the mean values of firing rate were calculated for each block respectively.

Offline Spike Detection and Spike Sorting

The digital signals were band-pass filtered between 0.5 and 5 kHz, and spikes were detected when the signal-to-noise ratio was over 2.0. For spike sorting, the voltage waveforms were aligned directly using a waveform peak. Spikes with similar waveforms were eyeballed and picked up as one cluster (one neuron), and the rest of waves with apparent differences from the cluster were eliminated.

For each neuron, raster plots were binned into 1 ms with a time window from 100 ms prior to the sound presentation to 300 ms after the presentation. The histograms were plotted in the same window but were binned every 5 ms. The firing rates during the 200-ms stimulus presentation time were used for the scatterplots.

Electrophysiological data collection and analysis programs were programmed with Labview (National Instruments) and displayed with Graphpad 5.1 (GraphPad Software).

Differentiated Neurons Auditory Response Activity Assessed with c-Fos Expression

After the electrophysiological experiments were finished, the monkeys were separated randomly into two groups and put in anechoic chambers. The first group, containing three monkeys, was placed individually in the chamber without sound stimuli for 2 hr prior to being exposed to a wide-band white-noise auditory stimulus (80 dB) for 30 min. Then, the monkeys were kept in the chamber without sound stimuli for another 90 min. The second group, containing two monkeys, was placed individually in the anechoic chamber without any sound stimuli for 4 hr. After the 4-hr periods, all animals were immediately sacrificed, and the brain tissues were fixed in 4% paraformaldehyde. Immunohistochemistry of c-*fos* was performed as described later. c-Fos-positive cells were counted using the CellSens Dimension software (Olympus).

Immunohistochemistry

The brains were collected and postfixed for 4 hr at 4°C, then they were cryoprotected in 30% sucrose and sectioned into 10-μm-thick slices. The slices were permeabilized with 0.2% Triton X-100 for 40 min and blocked with 5% BSA for 1 hr at room temperature. Slides were then incubated with primary antibodies at 4°C overnight. The sections were then washed three times and incubated with secondary antibodies for 2 hr at 37°C.

The transplanted cells were identified with GFP fluorescence. For different purposes, GFP-positive cells were later double stained with antibodies to Map2, NeuN, Tau, Synapsin I, PSD95, c-*fos*, and GFAP (glial fibrillary acidic protein). The sections were mounted with DAPI containing mounting solution. The slides were examined with an Olympus FV1000 fluorescence microscope. Information pertaining to the primary and secondary antibodies is presented in Tables S3 and S4, respectively.

Statistics

A t test was performed for c-*fos* immunohistochemical data with GraphPad Prism 5.1 (GraphPad Software). Significance was set at $p < 0.01$.

SUPPLEMENTAL INFORMATION

Supplemental Information includes five figures and five tables and can be found with this article online at http://dx.doi.org/10.1016/j.celrep.2016.06.066.

AUTHOR CONTRIBUTIONS

X.H., Z.W., S.Y., J.L., Y. Yao, and L. Xu initiated the project, designed the experiments, and wrote the manuscript. X.H. organized and supervised the whole project. Z.W. organized and supervised all monkey work. S.Y. organized and supervised the monkey model work. Z.W. performed the cell culture. Z.W., W.W., J. Wei, and R.Z. performed IC lesion model, single-neuron recording, and data analysis etc. Y.Z. collected data, wrote program codes, and performed data analysis. Y. Yin performed the monkey surgery. L. Li, L.X., and L. Liu performed the IC localization. Y.H., J. Wu, L.Y., H.L., D.Q., and X.F. assisted in monkey work. M.P. and A.G. edited the manuscript. J.R. provided advice and wrote and edited the manuscript. W.W., J. Wei, and R.Z. contributed equally to this work.

ACKNOWLEDGMENTS

We thank Dr. Robert Desimone from MIT and Dr. Gong Chen from PSU for their valuable suggestions on the manuscript. This research was supported by the National Program for Key Basic Research Project (973 Programs 2015CB755605, 2012CB825503, and 2012CBA01304), the Strategic Priority Research Program of CAS (XDB02020005), the Key Research Program of the Chinese Academy of Sciences, the Selected Frontier Scientific Significant Breakthrough Project of CAS, the Key Program of the Chinese Academy of Sciences (KZCC-EW-103-2), the Training Program of the Major Research Plan of the National Natural Science Foundation of China (91332120), the National Natural Science Foundation of China (81471312, 31271167, 81271495, and 81460352), the Yunnan Provincial Project to Attract One-hundred Exceptional Talents From Overseas, and the Applied Basic Research Programs of Science and Technology Commission Foundation of Yunnan Province (2014FA047).

Received: March 9, 2015
Revised: January 6, 2016
Accepted: June 15, 2016
Published: July 14, 2016

REFERENCES

Barone, F.C., and Feuerstein, G.Z. (1999). Inflammatory mediators and stroke: new opportunities for novel therapeutics. J. Cereb. Blood Flow Metab. *19*, 819–834.

Benninger, F., Beck, H., Wernig, M., Tucker, K.L., Brüstle, O., and Scheffler, B. (2003). Functional integration of embryonic stem cell-derived neurons in hippocampal slice cultures. J. Neurosci. *23*, 7075–7083.

Blurton-Jones, M., Kitazawa, M., Martinez-Coria, H., Castello, N.A., Müller, F.J., Loring, J.F., Yamasaki, T.R., Poon, W.W., Green, K.N., and LaFerla, F.M. (2009). Neural stem cells improve cognition via BDNF in a transgenic model of Alzheimer disease. Proc. Natl. Acad. Sci. USA *106*, 13594–13599.

Borisyuk, A., Semple, M.N., and Rinzel, J. (2002). Adaptation and inhibition underlie responses to time-varying interaural phase cues in a model of inferior colliculus neurons. J. Neurophysiol. *88*, 2134–2146.

Breunig, J.J., Haydar, T.F., and Rakic, P. (2011). Neural stem cells: historical perspective and future prospects. Neuron *70*, 614–625.

Englund, U., Bjorklund, A., Wictorin, K., Lindvall, O., and Kokaia, M. (2002). Grafted neural stem cells develop into functional pyramidal neurons and integrate into host cortical circuitry. Proc. Natl. Acad. Sci. USA *99*, 17089–17094.

Ferreira, A., and Rapoport, M. (2002). The synapsins: beyond the regulation of neurotransmitter release. Cell. Mol. Life Sci. *59*, 589–595.

Fuortes, M.G., Frank, K., and Becker, M.C. (1957). Steps in the production of motoneuron spikes. J. Gen. Physiol. *40*, 735–752.

Gutman, A., and Wasylyk, B. (1991). Nuclear targets for transcription regulation by oncogenes. Trends Genet. *7*, 49–54.

Hebb, D.O. (1949). The Organization of Behavior: A Neuropsychological Theory (Erlbaum).

Humphrey, D.R., and Schmidt, E.M. (1990). Extracellular single-unit recording methods. In Neurophysiological Techniques: Applications to Neural Systems, Alan A. Boulton, G.B. Baker, and Case H. Vanderwolf, eds. (Clifton, NJ: Humana Press), pp. 1–64.

Hunt, C.A., Schenker, L.J., and Kennedy, M.B. (1996). PSD-95 is associated with the postsynaptic density and not with the presynaptic membrane at forebrain synapses. J. Neurosci. *16*, 1380–1388.

Jing, W., Wenchao, W., Lin, L., Li, L., Guimei, W., Heng, T., Huihui, J., Jianhong, W., Yuanye, M., and Xintian, H. (2010). A new MRI approach for accurately implanting microelectrodes into deep brain structures of the rhesus monkey (Macaca mulatta). J. Neurosci. Methods *193*, 203–209.

Kelly, S., Bliss, T.M., Shah, A.K., Sun, G.H., Ma, M., Foo, W.C., Masel, J., Yenari, M.A., Weissman, I.L., Uchida, N., et al. (2004). Transplanted human fetal neural stem cells survive, migrate, and differentiate in ischemic rat cerebral cortex. Proc. Natl. Acad. Sci. USA *101*, 11839–11844.

Lu, P., Jones, L.L., Snyder, E.Y., and Tuszynski, M.H. (2003). Neural stem cells constitutively secrete neurotrophic factors and promote extensive host axonal growth after spinal cord injury. Exp. Neurol. *181*, 115–129.

McAlpine, D., Jiang, D., and Palmer, A.R. (2001). A neural code for low-frequency sound localization in mammals. Nat. Neurosci. *4*, 396–401.

Miyata, S., Tsujioka, H., Itoh, M., Matsunaga, W., Kuramoto, H., and Kiyohara, T. (2001). Time course of Fos and Fras expression in the hypothalamic supraoptic neurons during chronic osmotic stimulation. Brain Res. Mol. Brain Res. *90*, 39–47.

Pankratz, M.T., Li, X.J., Lavaute, T.M., Lyons, E.A., Chen, X., and Zhang, S.C. (2007). Directed neural differentiation of human embryonic stem cells via an obligated primitive anterior stage. Stem Cells *25*, 1511–1520.

Rosahl, T.W., Geppert, M., Spillane, D., Herz, J., Hammer, R.E., Malenka, R.C., and Südhof, T.C. (1993). Short-term synaptic plasticity is altered in mice lacking synapsin I. Cell *75*, 661–670.

Rossi, F., and Cattaneo, E. (2002). Opinion: neural stem cell therapy for neurological diseases: dreams and reality. Nat. Rev. Neurosci. *3*, 401–409.

Ryan, A., and Miller, J. (1978). Single unit responses in the inferior colliculus of the awake and performing rhesus monkey. Exp. Brain Res. *32*, 389–407.

Sahni, V., and Kessler, J.A. (2010). Stem cell therapies for spinal cord injury. Nat. Rev. Neurol. *6*, 363–372.

Schnupp, J.W., and King, A.J. (1997). Coding for auditory space in the nucleus of the brachium of the inferior colliculus in the ferret. J. Neurophysiol. *78*, 2717–2731.

Southwell, D.G., Nicholas, C.R., Basbaum, A.I., Stryker, M.P., Kriegstein, A.R., Rubenstein, J.L., and Alvarez-Buylla, A. (2014). Interneurons from embryonic development to cell-based therapy. Science *344*, 1240622.

Thuret, S., Moon, L.D., and Gage, F.H. (2006). Therapeutic interventions after spinal cord injury. Nat. Rev. Neurosci. *7*, 628–643.

van Praag, H., Schinder, A.F., Christie, B.R., Toni, N., Palmer, T.D., and Gage, F.H. (2002). Functional neurogenesis in the adult hippocampus. Nature *415*, 1030–1034.

Weick, J.P., Liu, Y., and Zhang, S.C. (2011). Human embryonic stem cell-derived neurons adopt and regulate the activity of an established neural network. Proc. Natl. Acad. Sci. USA *108*, 20189–20194.

Wernig, M., Benninger, F., Schmandt, T., Rade, M., Tucker, K.L., Büssow, H., Beck, H., and Brüstle, O. (2004). Functional integration of embryonic stem cell-derived neurons in vivo. J. Neurosci. *24*, 5258–5268.

Wianny, F., Bernat, A., Huissoud, C., Marcy, G., Markossian, S., Cortay, V., Giroud, P., Leviel, V., Kennedy, H., Savatier, P., and Dehay, C. (2008). Derivation and cloning of a novel rhesus embryonic stem cell line stably expressing tau-green fluorescent protein. Stem Cells *26*, 1444–1453.

Wu, J., Wang, W., Rizak, J.D., Wang, Z., Wang, J., Feng, X., Dong, J., Li, L., Liu, L., Xu, L., et al. (2014). A new method for piercing the tentorium cerebelli for implanting fragile electrodes into the brain stem in the rhesus monkey (Macaca mulatta). J. Neurophysiol. *111*, 1027–1032.

Zhou, F.W., Fortin, J.M., Chen, H.X., Martinez-Diaz, H., Chang, L.J., Reynolds, B.A., and Roper, S.N. (2015). Functional integration of human neural precursor cells in mouse cortex. PLoS ONE *10*, e0120281.

Zwiers, M.P., Versnel, H., and Van Opstal, A.J. (2004). Involvement of monkey inferior colliculus in spatial hearing. J. Neurosci. *24*, 4145–4156.

Cell Reports, Volume *16*

Supplemental Information

Neurons Differentiated from Transplanted Stem Cells Respond Functionally to Acoustic Stimuli in the Awake Monkey Brain

Jing-kuan Wei, Wen-chao Wang, Rong-wei Zhai, Yu-hua Zhang, Shang-chuan Yang, Joshua Rizak, Ling Li, Li-qi Xu, Li Liu, Ming-ke Pan, Ying-zhou Hu, Abdelaziz Ghanemi, Jing Wu, Li-chuan Yang, Hao Li, Long-bao Lv, Jia-li Li, Yong-gang Yao, Lin Xu, Xiao-li Feng, Yong Yin, Dong-dong Qin, Xin-tian Hu, and Zheng-bo Wang

Neurons Differentiated from Transplanted Stem Cells Respond Functionally to Acoustic Stimuli in the Awake Monkey Brain

Jing-kuan Wei[1, 6, 7], Wen-chao Wang[1, 6, 7], Rong-wei Zhai[1, 6, 7], Yu-hua Zhang[1], Shang-chuan Yang[1], Joshua Rizak[1], Ling Li[3], Li-qi Xu[3], Li Liu[3], Ming-ke Pan[1], Ying-zhou Hu[1], Abdelaziz Ghanemi[1], Jing Wu[1], Li-chuan Yang[1], Hao Li[1], Long-bao Lv[4], Jia-li Li[1], Yong-gang Yao[1, 2], Lin Xu[1, 2], Xiao-li Feng[1], Yong Yin[5], Dong-dong Qin[1], Xin-tian Hu[1, 2, 4, 8] , Zheng-bo Wang[1, 8]

[1] Key Laboratory of Animal Models and Human Disease Mechanisms of Chinese Academy of Sciences & Yunnan Province, Kunming Institute of Zoology, Kunming, Yunnan, 650223, China

[2] CAS Center for Excellence in Brain Science and Intelligence Technology, Chinese Academy of Sciences, Shanghai, 200031, China

[3] Kunming General Hospital of PLA Medical Imaging Department, Kunming, Yunnan, 650032, China

[4] Kunming Primate Research Center, Kunming Institute of Zoology, Chinese Academy of Sciences, Kunming, Yunnan, 650223, China

[5] Department of Rehabilitation Medicine, the Fourth Affiliated Hospital of Kunming Medical University, Kunming, Yunnan, 650021, China

[6] Kunming College of Life Science, University of Chinese Academy of Sciences, Kunming, Yunnan, 650204, China

[7] These authors contributed equally to this work.
[8] Correspondence: wangzb@mail.kiz.ac.cn (Z.W.), xthu@mail.kiz.ac.cn (X.H.)

Supplementary

Table S1. Related to Figure S3, 4. The size of the transplanted tissues in the five monkey IC.

Animals' ID	M09311	M07437	M07409	M07403	M08001	Average
Depth (mm)	2.77	2.02	2.64	2.22	3.02	2.53
Diameter (mm)	1.89	1.82	1.77	1.82	1.92	1.84
Electrode ending depth (mm)	1.0	1.0	0.906	1.0	1.5	N/A

Table S2. Related to Figure 4, 5 and 6. Electrophysiological data of all the neurons from the five monkeys.

Animal ID	M09311	M07437	M07409	M07403	M08001
Number of Total Neurons	9	1	1	3	5
Stimuli-Related Neurons	m09311-3*#^ m09311-4* m09311-5*^ m09311-8#			m07403-3#	
Spontaneous Discharge Neurons	m09311-1 m09311-2 m09311-6 m09311-7 m09311-9	m07437-1	m07409-1	m07403-1 m07403-2	m08001-1 m08001-2 m08001-3 m08001-4 m08001-5

The number after the animal ID is named in chronological order. For instance, 'm09311-3' was the third neuron recorded from M09311. '#' represents the response was frequency related. '*' represents intensity related. '^' represents an adaptive response.

Table S3. Related to Figure 2, 3 and Figure S5. Primary antibodies in alphabetical order.

Immunogen	Species/Class	Cat. No	Supplier	Dilution for ICC
c-fos	Rabbit/IgG	226 003	Synaptic system	1:200
GFAP	Mouse/IgG	SMI-21R	BioLegend	1:1000
Map2	Mouse/IgG1	M4403	Sigma	1:800
Nestin	Rabbit/IgG	AB5922	Millipore	1:200
NeuN	Mouse/IgG1	MAB377	Millipore	1:200
NeuN	Rabbit/IgG	ABN78	Millipore	1:200
Oct4	Rabbit/IgG	Ab18976	Abcam	1:200
PSD95	Mouse/IgG1	Ab2723	Abcam	1:500
Sox1	Rabbit/IgG	Ab87775	Abcam	1:800
Synapsin	Rabbit/IgG	S193	sigma	1:800
Tau	Mouse/IgG1	ab12357	Abcam	1:800
Tuj-1	Mouse/IgG1	MAB1637	Millipore	1:200

Table S4. Related to Figure 2, 3 and Figure S5. Secondary antibodies.

Name	Supplier	Dilution
Goat anti-mouse IgG-cy3	sigma	1:400
Goat anti-rabbit IgG-cy3	sigma	1:400
Goat anti-rabbit IgG CFL405	Jackson	1:200
Goat anti-mouse IgG-cy5	Jackson	1:200
Donkey anti-rabbit IgG-cy5	Jackson	1:200

Table S5. Related to Figure 2J and 3C.

Figure		N（animals）	n（slices）	Avg Cell Number	SD	SEM
Fig. 2I	DAPI	5	31	1548.6	210.98	37.89
	NeuN			186.4	71.72	12.88
Fig. 6C	c-Fos (Stim)	3	8	98.0	12.14	4.29
	c-Fos (NStim)	2	9	6.7	3.42	1.14

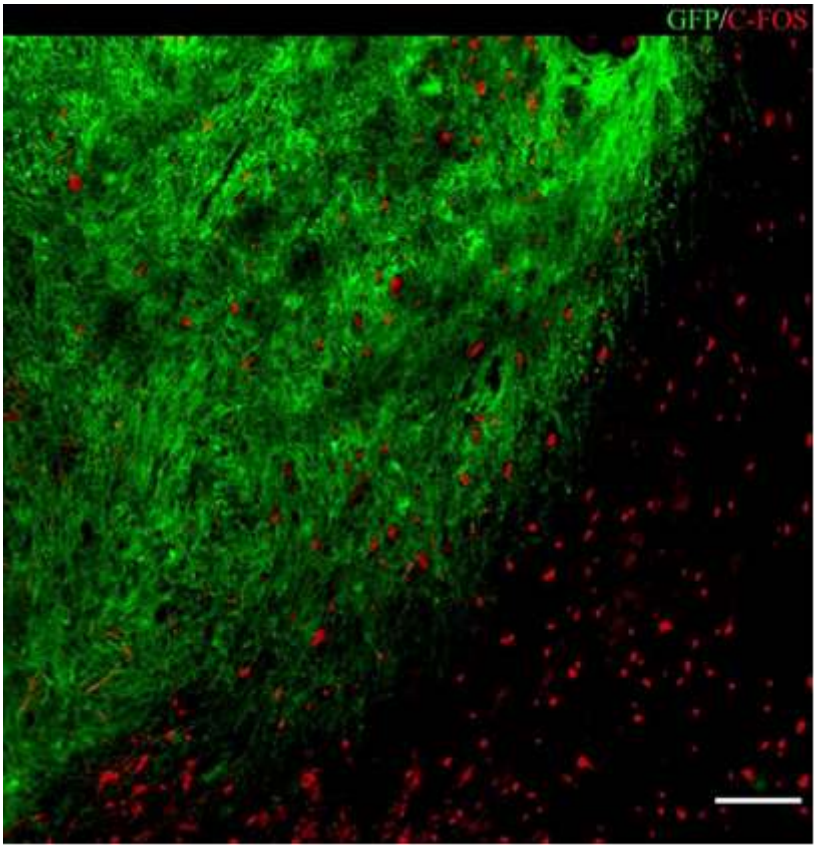

Figure S1. Related to Figure 3. The c-Fos expression in an auditory stimulated monkey. This figure shows both the transplanted area and nearby host brain area. The positive expression of c-Fos protein was about 2 fold higher in the host tissue than in the transplanted area. Scale bar: 100 μm.

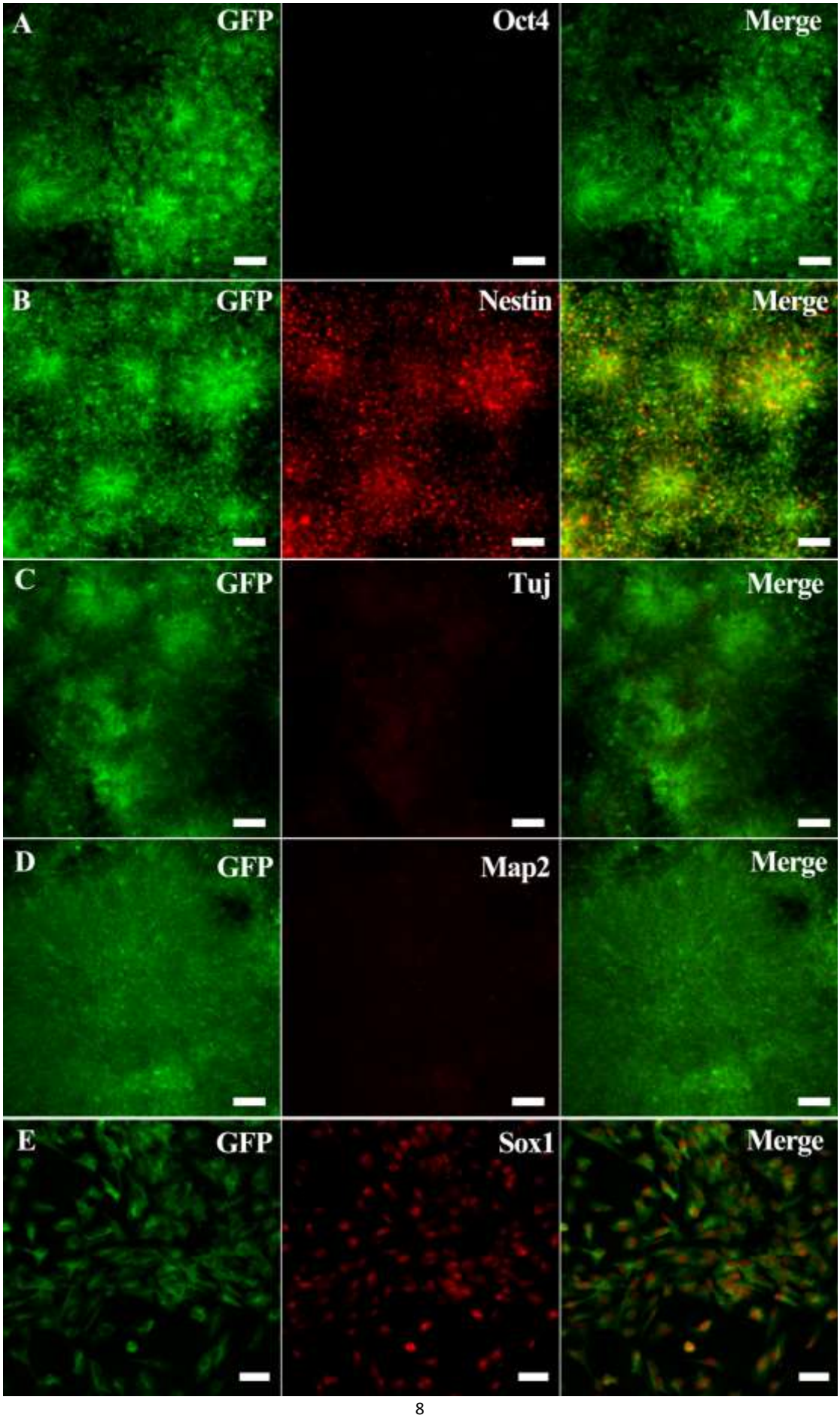
A
GFP
Oct4
Merge
B
GFP
Nestin
Merge
C
GFP
Tuj
Merge
D
GFP
Map2
Merge
E
GFP
Sox1
Merge

Figure S2. Related to Figure 1, 2. Immunocytochemistry tests for purity of NSCs.

(A) Oct4 was used to identify embryonic stem cells, and the image suggests there were almost no undifferentiated ESCs. **(B)** Nestin was used to identify NSCs, and the image suggests the majority of ESCs have differentiated into NSCs. **(C)** Beta tubulin III was used to identify neurons and the image suggests no NSCs have differentiated into neurons. **(D)** Map2 was used to identify neurons and no NSCs have differentiated into neurons. **(E)** After transplantation, Sox1 was used to identify NSCs from remaining cells and the result suggests most of cells were NSCs. Scale bars: 50 μm.

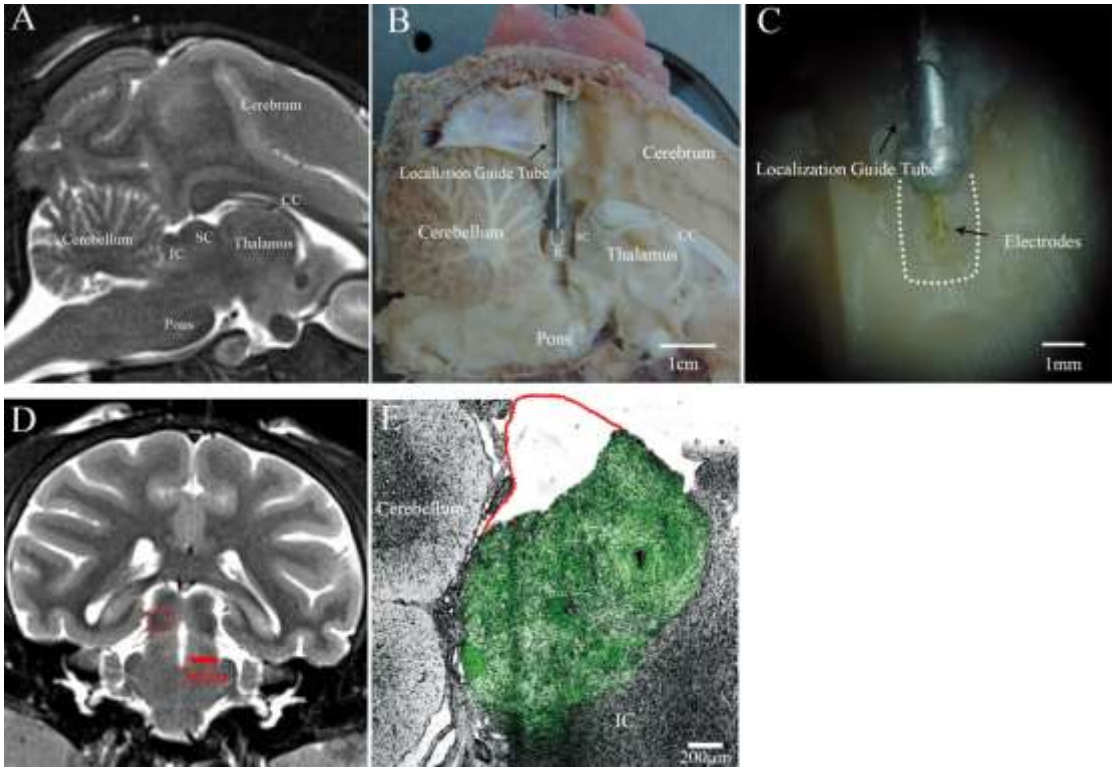

Figure S3. Related to Figure 1. MR images of the locations of IC, the electrode and a postmortem sagittal section of transplant tissue. (A) A sagittal MRI section shows the location of IC in the midbrain. **(B)** An actual photo of brain shows the location of the electrode is approximately at the same place as the IC in A. **(C)** An enlarged view of the electrode from B. The white dotted line shows the estimated area of the transplant site. **(D)** A coronal MRI section reveals IC size. The red circle indicates the left IC. The red bar is 5.00 mm in length. **(E)** A side view shows the location of the transplanted tissue, which is right next to the cerebellum and on the top of the IC. The red dotted line illustrates an estimated part of the transplanted tissue that was torn away when the electrode was taken out. SC, superior colliculus; CC, corpus callosum; IC, inferior colliculus.

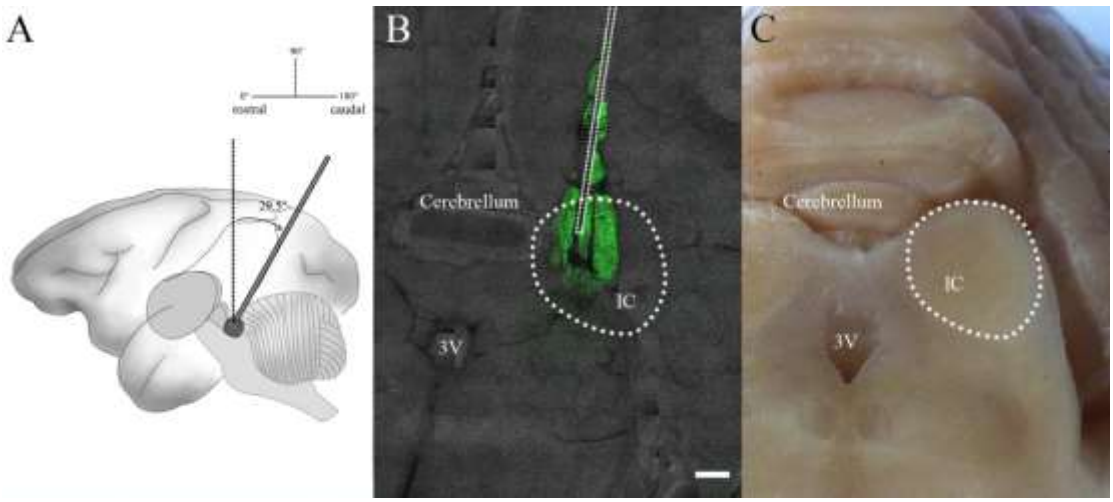

Figure S4. Related to Figure 1. Insertion angle of the Local Guide Tube and location of the transplanted tissue on the IC. (A) A schematic drawing shows the insertion angle of the localization guide tube, which was 29.5º to the posterior. **(B)** A coronal section cut at an angle tilted to the posterior by 29.5º (along the insertion track of the localization guide tube) shows the location of the transplanted tissue in the IC and the track of the electrode (white dotted line). The white dotted circle shows the estimated IC location which was identified by comparing B with C. Scale bar: 1 mm. **(C)** A coronal section of a brain stem cut at the same angle as a and b shows the location of IC relative to the third ventricle and cerebellum. This assisted with IC location in B. The telencephalon was detached from the brain stem in C, making the part differ from that of B The white dotted circle shows the IC area. 3V, third ventricle.

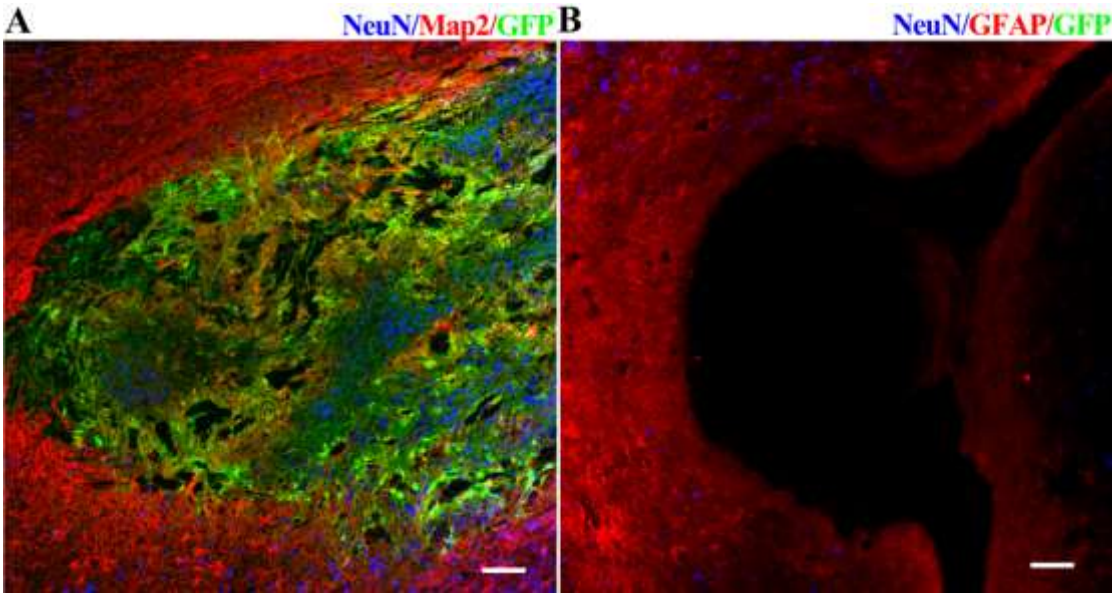

Figure S5. Related to Figure 2, 5 and 6. Comparison of the monkey IC histological sections from animals transplanted with GFP-neural stem cells and animals transplanted with monkey fibroblasts. (A) There are a substantial number of new neurons at the transplanted site in the IC in which GFP-neural stem cells had been transplanted. **(B)** No neurons or glial cells were found at the transplanted site of the IC in which monkey fibroblast cells had been transplanted. Antibodies in each image are marked above their corresponding image. Scale bar: 100 μm.